Bull. Chem. Soc. Jpn., **75**, 1637–1655 (2002)

Accounts

Electric Field Effects on Photochemical Dynamics in Solid Films

Nobuhiro Ohta

Research Institute for Electronic Science (RIES), Hokkaido University, Sapporo 060-0812

(Received November 20, 2001)

Electric field effects on photochemical dynamics have been examined with particular regard to photoinduced electron transfer (PIET) and excimer formation, based on the measurements of the field effects on emission spectra and emission decays. In various pairs of electron donor and acceptor and in their linked compounds, the following processes are shown to be significantly influenced by an electric field in a polymer film: the initial step of PIET, back-electron transfer which produces an fluorescent state, charge recombination, and dissociation of radical–ion pairs generated by PIET. With an oriented molecular system where vectorial interlayer PIET occurs, PIET is shown to be controlled by an electric field; the rate is depressed or enhanced by an electric field, depending on the field direction relative to the direction of the electron transfer. Electric field effects on excimer formation processes suggest that not only the level shift but also the change in orbital overlap between different chromophores play an significant role in electric field effects on photochemical dynamics.

A photochemical process such as photoinduced electron transfer, proton transfer or molecular complex formation usually depends on the electronic structure and level structure in the excited states. In order to elucidate the relation between dynamics and structure, observation of the change in dynamics will be essential in the presence of some external perturbation whose influence in structure can be well estimated. Such an approach may lead to a new way to control the photochemical reaction.

A shift of the molecular energy level induced by an external electric field is well known as the so-called Stark shift, and this effect has been extensively applied in molecular spectroscopy to examine the electronic structure in the excited state.[1–4] Therefore, application of external electric fields seems to induce a significant change in photochemical dynamics, as a result of the field-induced change in level structure of the excited molecules.[5–7] An applied magnetic field is another typical perturbation, which induces the so-called Zeeman shift, and the magnetic field effects on photochemical processes have been extensively examined.[8–11] It is likely that the magnitude of the level shift which can be induced by an external electric field is larger than that induced by an applicable magnetic field. Further, electric field effects on photochemical dynamics seem to be related to a photoinduced function of materials such as photoconductivity, nonlinear optical property or the generation of electroluminescence. However, the significance of the electric fields in enhancement or de-enhancement of the primary processes of photochemical reactions has not been referred to as much as the magnetic field effects especially in condensed phase.

Electric field effects on photochemical dynamics have been examined with particular regard to the field effects on photoinduced electron transfer and excimer formation, based on the measurements of the field-induced change in emission spectra, emission quantum yield and emission decays. Hereafter, photoinduced electron transfer is abbreviated as PIET. Electric field effects on PIET may be expected in two mechanisms: one is the field effects on the initial step of electron transfer and the other is the effect on dissociation or recombination process of the radical–ion pairs produced by PIET. The latter field effect, which competes with the Coulomb attraction and Brownian motion of radical–ion pairs, has been examined already, in relation to the photocarrier generation.[12–25] On the other hand, the study on the former effect is quite limited except for the field effect on the charge separation process in photosynthetic reaction centers.[26]

When electron donor (D) and acceptor (A) molecules are randomly distributed in three dimensional space, the analysis of the field effect is quite complicated, even if the field effect exists, since different pairs of D and A will show different magnitudes of field effects. If D and A can be arranged with a well defined molecular order, where PIET occurs with a definite direction, the mechanism of PIET and its field dependence may be elucidated much more clearly since the direction of PIET relative to the field direction can be well defined. The Langmuir–Blodgett (LB) technique can be used to prepare such a molecular assembly,[27,28] and the electrochromism has been successfully applied to the LB films in order to study electric properties of the embedded chromophores or layer structures.[29–35]

Photoexcitation dynamics of chain molecules, where two reactants are attached to chain ends, is also highly interesting, because of the fixed distance of two chromophores and of the through-bond interaction between two chromophores.[36–39] Therefore, electric field effects on fluorescence of linked compounds have been also examined.

In the present review, electric field effects on PIET are reported for a mixture of D and A molecules which are separately doped in a polymer solid film and for their linked compounds similarly doped in a polymer film. Electric field effects on interlayer vectorial PIET, which have been examined with LB multilayer films, and on excimer formation process, which have been examined for pyrene doped in a polymer film, are also reported.

Principle

When an electric field is applied to molecules, each energy level is in general shifted, and the magnitude of each shift depends on the electric dipole moment ($\boldsymbol{\mu}$) and the molecular polarizability ($\boldsymbol{\alpha}$) of the state concerned; the level shift is given by $-\boldsymbol{\mu F} - \boldsymbol{\alpha F}^2/2$, where $\boldsymbol{F}$ represents the external electric field. As a result, the transition energy for absorption as well as for emission is changed in the presence of an electric field. Hereafter, applied electric field is denoted by $\boldsymbol{F}$. For an isotropic and immobilized sample, the presence of $\boldsymbol{F}$ will broaden an isolated transition due to the change in electric dipole moment following absorption transition, giving rise to a Stark effect line shape which is approximately the second derivative of the absorption spectrum (see Fig. 1). If the change in molecular polarizability following photoexcitation is significant, the Stark effect line shape is the first derivative of the absorption spectrum. If the transition moment is affected by $\boldsymbol{F}$, the Stark effect line shape is the same as the absorption spectrum. By assuming that the original isotropic distribution is maintained even in the presence of $\boldsymbol{F}$, the change in absorption intensity at wavenumber, ν, in the presence of $\boldsymbol{F}$, i.e., $\Delta A(\nu)$, may be given by the following equation:[4,40,41]

$$\Delta A(\nu) = (f\boldsymbol{F})^2[\mathrm{A}A(\nu) + \mathrm{B}\nu\{\mathrm{d}(A(\nu)/\nu)/\mathrm{d}\nu\} + \mathrm{C}\nu\{\mathrm{d}^2(A(\nu)/\nu)/\mathrm{d}\nu^2\}] \quad (1)$$

where f is the internal field factor. The coefficient A depends on the transition moment polarizability and hyperpolarizability, and B and C are given as follows:

$$\mathrm{B} = [\Delta\bar{\alpha}/2 + (\Delta\alpha_{\mathrm{m}} - \Delta\bar{\alpha})(3\cos^2\chi - 1)/10]/(hc) \quad (2)$$

$$\mathrm{C} = (\Delta\mu)^2\,[5 + (3\cos^2\xi - 1)(3\cos^2\chi - 1)]/(30h^2c^2) \quad (3)$$

where h is the Planck's constant and c is the light speed. Here, $\Delta\mu$ and $\Delta\alpha$ are the differences in electric dipole moment and molecular polarizability, respectively, between the ground state (g) and the excited state (e), i.e., $\Delta\boldsymbol{\mu} = \boldsymbol{\mu}_{\mathrm{e}} - \boldsymbol{\mu}_{\mathrm{g}}$, and $\Delta\boldsymbol{\alpha} = \boldsymbol{\alpha}_{\mathrm{e}} - \boldsymbol{\alpha}_{\mathrm{g}}$:

$$\Delta\mu = |\Delta\boldsymbol{\mu}|;\ \Delta\bar{\alpha} = (1/3)\mathrm{Tr}(\Delta\boldsymbol{\alpha}) \quad (4)$$

$\Delta\alpha_{\mathrm{m}}$ denotes the diagonal component of $\Delta\boldsymbol{\alpha}$ with respect to the direction of the transition dipole moment, χ is the angle between the direction of F and the electric vector of the excitation light, and ξ is the angle between the direction of $\Delta\boldsymbol{\mu}$ and the transition dipole moment. The value of $\Delta\mu$ or $\Delta\bar{\alpha}$ can be easily obtained from the analysis of the derivative parts of the electroabsorption spectra.[42–46]

The electric field-induced change in fluorescence intensity, i.e., $\Delta I_{\mathrm{F}}(\nu)$, observed at the second harmonic of the modulation frequency in a polymer film, where molecules are randomly distributed, may be also given by an equation similar to Eq. 1, i.e., by a linear combination of the fluorescence spectrum and its first and second derivative spectra as follows:

$$\Delta I_{\mathrm{F}}(\nu) = (f\boldsymbol{F})^2[\mathrm{A}'I_{\mathrm{F}}(\nu) + B'\nu^3\{\mathrm{d}(I_{\mathrm{F}}(\nu)/\nu^3)/\mathrm{d}\nu\} + \mathrm{C}'\nu^3\{\mathrm{d}^2(I_{\mathrm{F}}(\nu)/\nu^3)/\mathrm{d}\nu^2\}] \quad (5)$$

The first and the second derivative components correspond to the spectral shift and the spectral broadening resulting from the difference in molecular polarizability and electric dipole moment between the fluorescent state and the ground state, respectively.[47,48] Here, a perfectly isotropic distribution of the emitting molecules is assumed, though this assumption may be not always valid.[49]

Let us consider the extreme system where no nonradiative process occurs, and the excited molecules dissipate excitation energy only through the emissive processes. In such a case, the emission intensity does not change even in the presence of $\boldsymbol{F}$, as far as the numbers of the excited molecules are the same. Even when the transition dipole moment is changed by $\boldsymbol{F}$, the fluorescence quantum yield (intensity) is not affected by $\boldsymbol{F}$, although the fluorescence lifetime is changed. When a molecule is excited, it always comes down to the ground state through emissive processes. When a nonradiative process competes

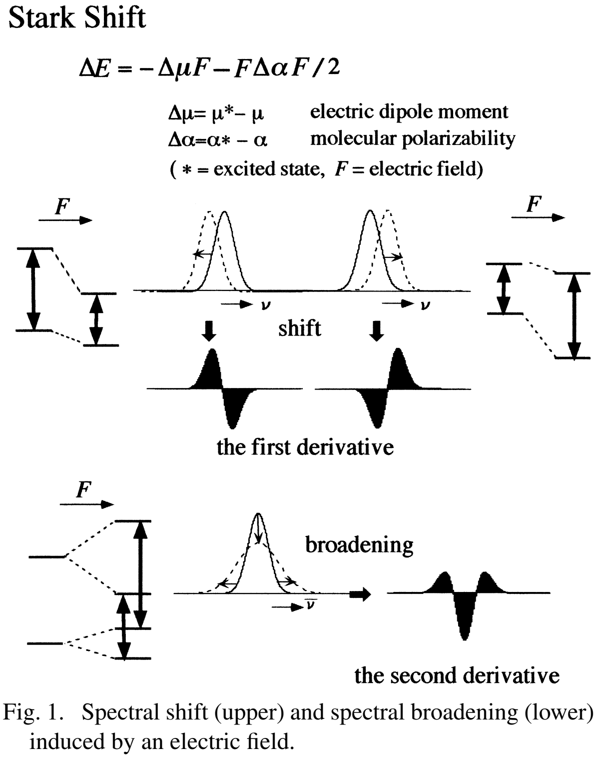

Fig. 1. Spectral shift (upper) and spectral broadening (lower) induced by an electric field.

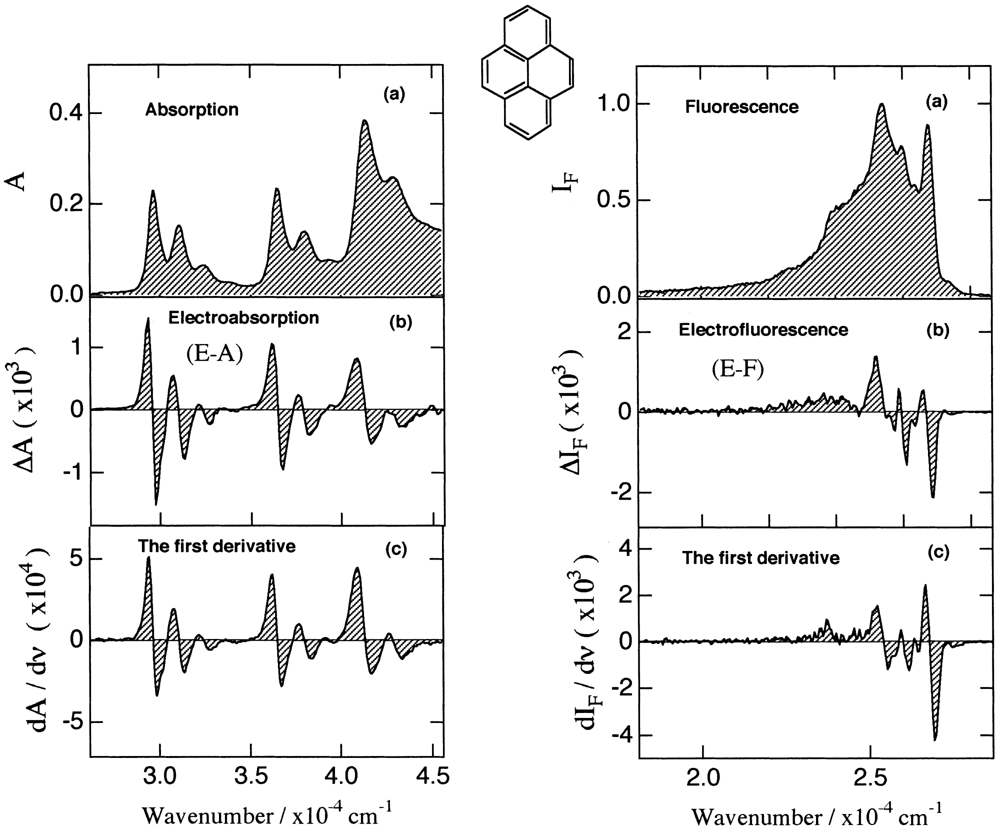

Fig. 2. Absorption spectrum, E-A spectrum and the first derivative of the absorption spectrum (left, from top to bottom), and fluorescence spectrum, E-F spectrum and the first derivative of the fluorescence spectrum (right, from top to bottom) of pyrene doped in a PMMA film at a concentration of 1.0 mol%. Excitation for fluorescence was at 322.0 nm. Intensity is given in arbitrary units in every case.

with the emissive processes, on the other hand, the field-induced change in transition dipole moment as well as in nonradiative process will induce a change in fluorescence intensity. Therefore, the component of $\Delta I_F(\nu)$ which gives the same shape as the emission spectrum, i.e., the first term in Eq. 5, corresponds to the field-induced change in emission quantum yield. Hence, the evaluation of the magnitude of the change in emission intensity, i.e., A′ in Eq. 5 provides us with information about the electric field effects on excitation dynamics.

As an example of the typical spectra of $\Delta A(\nu)$ or $\Delta I_F(\nu)$ which show the Stark shift, the observed spectra of pyrene doped in a PMMA film are shown in Fig. 2. Both spectra are essentially the same in shape as the first derivative of the absorption or fluorescence spectrum, indicating that the field-induced change in absorption or fluorescence intensity essentially comes from the change in molecular polarizability following absorption or emission. Because of the D_{2h} symmetry, isolated molecules of pyrene have no permanent electric dipole moment, and so it is well understood that $\Delta\mu$ is zero at a low concentration of pyrene in PMMA films. The fact that the signal intensity of $\Delta A(\nu)$ relative to the first derivatives of the absorption spectrum decreases, as the excited state becomes higher, indicates that the magnitude of $\Delta\bar{\alpha}$ depends on the electronic states to which transition occurs.[50] Plots of ΔA or ΔI_F as a function of wavenumber or wavelength are called electroabsorption spectrum and electrofluorescence spectrum, respectively; these are hereafter abbreviated as E-A and E-F spectra, respectively.

In an oriented system where molecules are arranged with a well-defined order, the change in absorption intensity or in emission intensity which is linearly proportional to the applied field strength will be significant, in contrast with the randomly distributed system. Therefore, the field-induced change in absorption or emission intensity may be observed at the first harmonic of the modulation frequency, and E-A spectra or E-F spectra may be given by a linear combination between the absorption or emission spectrum and its first derivative spectrum.[32–34,51] The first derivative part corresponds to the Stark shift induced by a nonzero value of $\Delta\mu$ in both spectra. On the other hand, E-F spectrum which gives the same shape as the fluorescence spectrum corresponds to the field-induced change in emission quantum yield, while E-A spectra which give the same shape as the absorption spectrum results from the transition moment polarizability. In an oriented system, therefore, field-induced changes in excitation dynamics can be examined by measuring the E-F spectra at the first harmonic of the modulation frequency.

Experimental

Polymer films of poly(methyl methacrylate) (PMMA) where dye chromophores are randomly distributed and multistacking LB films were used as solid thin films. Following the cast of the polymer film on ITO-coated quartz plate or on semi-transparent aluminum film, a semi-transparent aluminum (Al) film is deposited on the film. Following the deposition of the LB multilayer films on semi-transparent Al film, a semi-transparent Al film is also deposited. The aluminum films and ITO films were used as electrodes. The thickness of the polymer films was determined directly using the measurement system, while total thicknesses of the LB films were calculated by assuming that the thickness of each LB monolayer film of palmitic acid, stearic acid, arachidic acid, and behenic acid is 22.4, 25.0, 27.3, and 29.9 Å, respectively.[52]

All the optical measurements were carried out at room temperature under vacuum conditions. A sinusoidal ac voltage was applied between the electrodes. A small amount of ac component of transmitted excitation light intensity or emission intensity at wavelength λ, $\Delta I(\lambda)$, synchronized with the applied voltage, was detected with a lock-in amplifier at the first harmonic of the modulation frequency in LB multilayer films and at the second harmonic of the modulation frequency in polymer films. A dc component of the transmitted light intensity or the total emission intensity at λ, $I(\lambda)$, was simultaneously obtained. The procedures have been described in detail elsewhere.[32,50] E-A spectra were obtained from $-\Delta \boldsymbol{I}(\lambda)/2.303\boldsymbol{I}(\lambda)$. In the measurements of the E-F spectra, excitation was done at the wavelengths where $\Delta \boldsymbol{A}(\nu)$, i.e., $\Delta \boldsymbol{A}(\lambda)$, is negligibly small.

The strength of $\boldsymbol{F}$, which was determined by dividing the applied voltage by the total thickness of the solid films, is represented in rms value. Usually, the internal electric field ($\boldsymbol{F}_{\text{int}}$) is not the same as the applied field, $\boldsymbol{F}$, because of the dielectric properties of the environment, but the relation between these two may be regarded as $\boldsymbol{F}_{\text{int}} = f\boldsymbol{F}$ (see Eqs. 1 and 5).

Fluorescence decays were measured by using a picosecond or femtosecond pulse laser and a single-photon-counting system equipped with a microchannel plate photomultiplier.[53]

Results and Discussion

1. Photoinduced Electron Transfer (PIET). Energy levels of the radical–ion pairs produced by PIET are expected to be significantly affected by $\boldsymbol{F}$ because of their large electric dipole moments. It is also expected that electric fields induce a change in overlap between the wavefunctions of the initial and final states of the electron transfer because of the field-induced orbital polarization. Consequently, electric fields may induce a remarkable change in the rate of the initial step of PIET, since the processes of PIET are considered to depend on the free energy gap between reactant and product and on the electronic coupling between donor and acceptor (see Fig. 3).[54–56] By measuring the electric field dependence of the fluorescence properties, we can examine field effects on PIET both in a randomly distributed system and in a well-oriented molecular system.

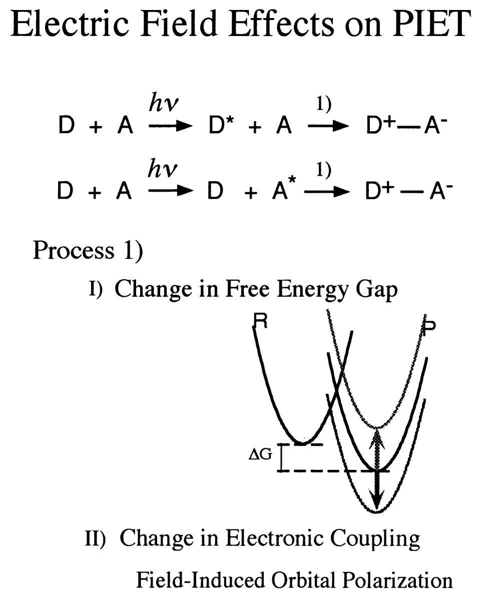

Fig. 3. Photoinduced electron transfer (PIET) and the possible mechanism of the field-induced change in the initial step of electron transfer.

a) Random Distribution of a Mixture of Donor (D) and Acceptor (A). The initial step of PIET is influenced by $\boldsymbol{F}$ in a mixture of D and A molecules separately doped in a polymer film. At first, the results of a mixture of *N*-ethylcarbazole and dimethyl terephthalate, denoted by ECZ and DMTP respectively, are described.[57] Fluorescence spectra and E-F spectra of a mixture of ECZ and DMTP doped in a PMMA film are shown in Fig. 4, where the ECZ concentration is 1.0 mol% in every case. In addition to the sharp fluorescence emitted from the locally excited state of ECZ, broad exciplex fluorescence appears with a peak at ~440 nm, as a result of PIET from the excited state of ECZ to DMTP, as the DMTP concentration increases. Hereafter, the sharp structured fluorescence is referred to as ECZ fluorescence or LE fluorescence. The E-F spectrum observed in the absence of DMTP is nearly identical with the first derivative of the fluorescence spectrum, indicating that the field effect on the ECZ fluorescence in the absence of DMTP results from the so-called Stark shift. As the DMTP concentration increases, the E-F spectrum in the shorter wavelength region becomes closer in shape to the ECZ fluorescence spectrum. The negative value of $\Delta I_{\text{F}}(\lambda)$ of the ECZ fluorescence shows that the quantum yield of the ECZ fluorescence is reduced by $\boldsymbol{F}$ in the presence of DMTP. Actually, the observed E-F spectra of ECZ are well reproduced by a linear combination of the fluorescence spectrum with its first derivative spectrum. The former, which gives a shape similar to the fluorescence spectrum, is attributed to the field-induced change in fluorescence quantum yield ($\Delta \Phi_{\text{F}}$), while the first derivative term corresponds to the Stark shift induced by a nonzero value of $\Delta\bar{\alpha}$ between the fluorescent state and the ground state.

Time-resolved fluorescence intensity, $I_{\text{F}}(t)$, observed for the ECZ fluorescence in the absence of DMTP shows a nearly single exponential decay, and its lifetime (τ_{F}^0) is determined to be 12.5 ns. Here, t presents the time. In the presence of DMTP, ECZ fluorescence shows a nonexponential decay, suggesting that ECZ molecules doped in a film interact with each other in various manners. The average lifetime of fluorescence, denoted by $\bar{\tau}_{\text{F}}$, was determined with the following equation: $\bar{\tau}_{\text{F}} = \int I_{\text{F}}(t)dt/I_{\text{F}}(0)$.[58] $\bar{\tau}_{\text{F}}$ of the ECZ fluorescence at 1.0 mol% obtained with various concentrations of DMTP shows that the average lifetime monotonically decreases with increasing DMTP concentration. Then, the average rate constant of

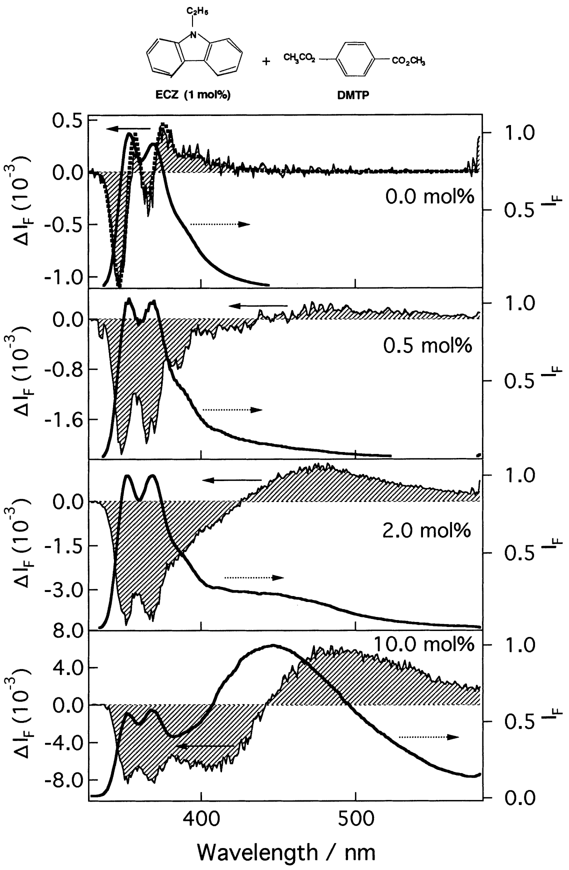

Fig. 4. Fluorescence spectra (solid line) and E-F spectra of a mixture of ECZ and DMTP doped in a PMMA film. The concentration of DMTP was 0, 0.5, 2.0, and 10.0 mol% from top to bottom, while the ECZ concentration was 1.0 mol% in every case. Applied field strength was 0.6 MV cm^{-1}, and excitation wavelength was 294 nm. The maximum fluorescence intensity is normalized to unity in every case. The first derivative of the fluorescence spectrum is also shown by a dotted line in the top.

the electron transfer from photoexcited ECZ to DMTP, k_{et}, is evaluated by using the following equation: $k_{\mathrm{et}} = 1/\bar{\tau}_{\mathrm{F}} - 1/\tau_0$. As shown in Fig. 5, the rate of PIET from the excited state of ECZ to DMTP, i.e., k_{et}, increases with decreasing D–A distance, i.e., R. Note that R is inversely proportional to $c^{1/3}$, where c is the DMTP concentration. Usually, k_{et} depends on R exponentially,[37,56,59] but the present results show that k_{et} increases multiexponentially with decreasing R.

A field-induced change in quantum yield of the ECZ fluorescence is considered to be caused by a field-induced change in k_{et}, i.e, Δk_{et}. The quantum yield of the ECZ fluorescence at zero field and its field-induced change are denoted by Φ_{F} and $\Delta\Phi_{\mathrm{F}}$, respectively. If one assumes that the relaxation processes of the photoexcited molecule of ECZ are irreversible, Φ_{F} and $\Phi_{\mathrm{F}} + \Delta\Phi_{\mathrm{F}}$ are given by $k_{\mathrm{r}}/(k_{\mathrm{r}} + k_{\mathrm{nr}} + k_{\mathrm{et}})$ and $k_{\mathrm{r}}/(k_{\mathrm{r}} + k_{\mathrm{nr}} + k_{\mathrm{et}} + \Delta k_{\mathrm{et}})$, respectively. Here, k_{r} and k_{nr} represent the rate constants of radiative processes and of nonradiative processes other than the electron transfer, respectively. By assuming that $\bar{\tau}_{\mathrm{F}}$ is given by $1/(k_{\mathrm{r}} + k_{\mathrm{nr}} + k_{\mathrm{et}})$, Δk_{et} is related to $\Delta\Phi_{\mathrm{F}}/\Phi_{\mathrm{F}}$ and $\bar{\tau}_{\mathrm{F}}$ by the following equation:

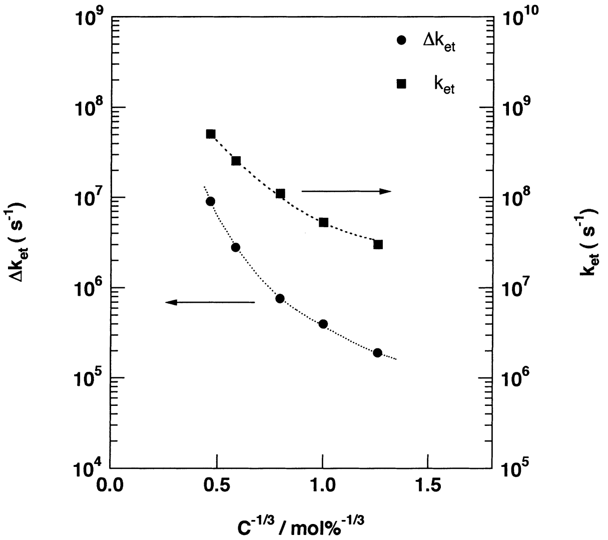

Fig. 5. Plots of k_{et} (■) and Δk_{et} (●) for a mixture of ECZ and DMTP as a function of the inverse cube root of DMTP concentration. ECZ concentration was 1.0 mol%, and applied field strength was 0.6 MV cm^{-1}.

$$\Delta k_{\mathrm{et}} = -(\Delta\Phi_{\mathrm{F}}/\Phi_{\mathrm{F}})/[\{1 + (\Delta\Phi_{\mathrm{F}}/\Phi_{\mathrm{F}})\}\,\bar{\tau}_{\mathrm{F}}] \tag{6}$$

The values of Δk_{et} evaluated with Eq. 6 are shown in Fig. 5 as a function of $c^{-1/3}$, together with k_{et}. Δk_{et} also increases monotonically with decreasing donor–acceptor distance, i.e., R.

According to the classical theory,[54,55] the rate constant of electron transfer is given by

$$k_{\mathrm{et}} = \frac{2\pi}{\hbar}\frac{J^2}{(4\pi k_{\mathrm{B}}T\lambda_0)^{1/2}}\exp[-\frac{(\Delta G+\lambda_0)^2}{4k_{\mathrm{B}}T\lambda_0}] \tag{7}$$

Here, J, $\hbar$, k_{B}, T, and ΔG are the transfer integral, Planck's constant divided by 2π, the Boltzmann constant, temperature, and free energy gap of the reaction, respectively, and λ_0 is the so-called reorganization energy. The external electric field is regarded as a perturbation, and the electron transfer rate can be expanded as a power series in $\boldsymbol{F}$. Hereafter, the zeroth, the first and the second order terms in $\boldsymbol{F}$ are considered, and other higher terms are neglected. It is assumed that only ΔG is affected by $\boldsymbol{F}$. Then, ΔG is replaced by $\Delta G_0 - \boldsymbol{\mu F}$, where ΔG_0 is the free energy gap in the absence of $\boldsymbol{F}$ and $\boldsymbol{\mu}$ is the dipole moment of the produced radical–ion pair.

The values of k_{et} in the presence and absence of $\boldsymbol{F}$ are denoted to be $k_{\mathrm{et}}(\boldsymbol{F})$ and $k_{\mathrm{et}}(\boldsymbol{F} = 0)$, respectively. By assuming that the rate constant of PIET in a polymer film is given by Eq. 7, Δk_{et}, which is defined as $k_{\mathrm{et}}(\boldsymbol{F}) - k_{\mathrm{et}}(\boldsymbol{F} = 0)$, divided by $k_{\mathrm{et}}(\boldsymbol{F} = 0)$ is given by

$$\begin{aligned}\Delta k_{\mathrm{et}}/k_{\mathrm{et}}(\boldsymbol{F} = 0) &= -2\mathrm{D}(\Delta G_0 + \lambda_0)(\boldsymbol{\mu F}) \\ &\quad + \mathrm{D}\{1 + 2\mathrm{D}(\Delta G_0 + \lambda_0)^2\}(\boldsymbol{\mu F})^2\end{aligned} \tag{8}$$

where $\mathrm{D} = -(4k_{\mathrm{B}}T\lambda_0)^{-1}$.

In a polymer film where the sample is regarded as randomly distributed, the average value of $\boldsymbol{\mu F}$ and $(\boldsymbol{\mu F})^2$ integrated over the full space is given by zero and $|\boldsymbol{\mu}|^2|\boldsymbol{F}|^2/3$, respectively. Then, Eq. 8 can be rewritten as

$$\Delta k_{\mathrm{et}}/k_{\mathrm{et}}(\boldsymbol{F}=0) = \mathrm{D}\{1 + 2\mathrm{D}(\Delta G_0 + \lambda_0)^2\}(|\boldsymbol{\mu}|^2|\boldsymbol{F}|^2/3) \quad (9)$$

When $1 >> (\Delta\Phi_{\mathrm{F}}/\Phi_{\mathrm{F}})$, Δk_{et} is nearly proportional to $\Delta\Phi_{\mathrm{F}}$ according to Eq. 6, and Δk_{et} is expected to be proportional to $|\boldsymbol{F}|^2$. In fact, the quadratic field strength dependence of the field-induced change in fluorescence intensity was observed for the ECZ fluorescence; $\Delta\Phi_{\mathrm{F}}/\Phi_{\mathrm{F}} \propto \boldsymbol{F}^2$. The direct measurement of the field dependence of the fluorescence decay rate as well as theoretical treatment also shows the quadratic field strength dependence of the decay rate.[60,61]

Both Δk_{et} and k_{et} increase monotonically with decreasing D–A distance, i.e., R, as shown in Fig. 5. The value of R is estimated at each concentration of DMTP with the specific gravity of 1.19 for PMMA.[62] For example, R is estimated to be 9 Å and 7 Å at 5 and 10 mol% of DMTP, respectively. The radii of D and A are assumed to be 3 Å. By adopting the data of Δk_{et} and $k_{\mathrm{et}}(\boldsymbol{F} = 0)$ to Eq. 9, ΔG_0 is estimated to be -0.7 eV for PIET from ECZ to DMTP, which shows the validity of Eq. 9. In other words, the electric field effect on the ECZ fluorescence in a mixture of ECZ and DMTP could be interpreted in terms of the field-induced change in the free energy gap between reactant and product by assuming that ΔG_0 is -0.7 eV.

Tachiya and Murata[63] reported that the D–A distance dependence of k_{et} results from the interplay of the distance dependence of J and λ_0 and depends on the magnitude of ΔG_0. According to their calculations, k_{et} decreases monotonically with decreasing R when ΔG_0 is relatively large. On the other hand, k_{et} was shown to have a maximum at a certain distance, when ΔG_0 is small. The fact that k_{et} increases multiexponentially with decreasing R, observed in the present experiments, is predicted theoretically for the case where ΔG_0 is quite large.

In contrast with the ECZ fluorescence, exciplex fluorescence is slightly enhanced by $\boldsymbol{F}$, and the magnitude of $\Delta\Phi_{\mathrm{F}}/\Phi_{\mathrm{F}}$ is nearly independent of the DMTP concentration, as far as the ECZ concentration is as low as 1 mol%. Actually, E-F spectra of the exciplex fluorescence are reproduced by a linear combination between the exciplex fluorescence spectrum and its first derivative spectrum. The former corresponds to the field-induced change in Φ_{F}, while the latter corresponds to the Stark shift.

Fluorescent exciplex composed of ECZ and DMTP is assumed to be formed through the radical-ion pair state following the electron transfer from photoexcited ECZ to DMTP, as proposed for poly(vinylcarbazole) (PVCz) where an electron acceptor is doped.[13,14] Field-induced increase of k_{et} may increase the formation yield of the radical–ion pair. As a result, exciplex fluorescence may be enhanced. The enhancement may also result in part from the field-induced inhibition of the charge recombination process since the exciplex fluorescence quenched as a result of the charge recombination of the radical-ion pair may be recovered in the presence of $\boldsymbol{F}$. In fact, the charge recombination is inhibited in the presence of $\boldsymbol{F}$, as mentioned for D–A linked compounds.

ECZ fluorescence is quenched by $\boldsymbol{F}$, but exciplex fluorescence is always enhanced by $\boldsymbol{F}$, as far as the ECZ concentration is low. When the ECZ concentration is high, however, the field effects on exciplex fluorescence are very different from the ones at low concentrations,[19] as shown in Fig. 6. With high concentrations of ECZ, exciplex fluorescence is efficiently quenched in the presence of $\boldsymbol{F}$. These results remind us of a similar quenching of exciplex fluorescence observed in PVCz with an electron acceptor, where the quenching is attributed to the field-assisted dissociation of radical–ion pairs.[12–14] The fluorescence spectrum itself is roughly the same both for a mixture of ECZ (1 mol%) + DMTP (10 mol%) and for ECZ (10 mol%) + DMTP (1 mol%); the intensity of the exciplex fluorescence relative to the ECZ fluorescence is roughly the same in both spectra, implying that the efficiencies of the electron transfer in both samples are roughly the same. Thus, there

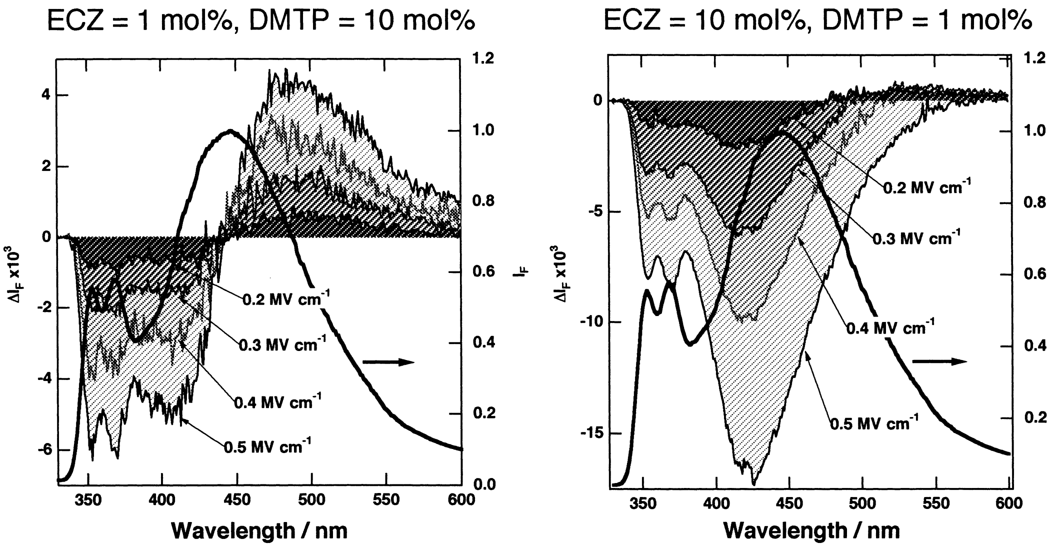

Fig. 6. Fluorescence spectra (solid line) and E-F spectra for a mixture of ECZ and DMTP observed with different field strengths. The concentrations of ECZ and DMTP were 1.0 and 10.0 mo% in the left, respectively, and 10.0 and 1.0 mol% in the right, respectively. The maximum fluorescence intensity is normalized to unity.

is no doubt that the efficiency of PIET does not decide whether exciplex fluorescence is quenched or enhanced in the presence of ***F***. The quenching of the exciplex fluorescence at high concentrations of ECZ is attributed to an efficient hole mobility, as will be mentioned later.

E-F spectra both of the ECZ fluorescence and of the exciplex fluorescence can be reproduced by a linear combination between the fluorescence spectrum and its first derivative spectrum at any concentrations. The former gives $\Delta\Phi_F$, while the latter results from the Stark shift induced by a non-zero value of $\Delta\overline{\alpha}$ following the fluorescing process. The observed field effects on fluorescence are interpreted in terms of Reaction in Scheme 1.

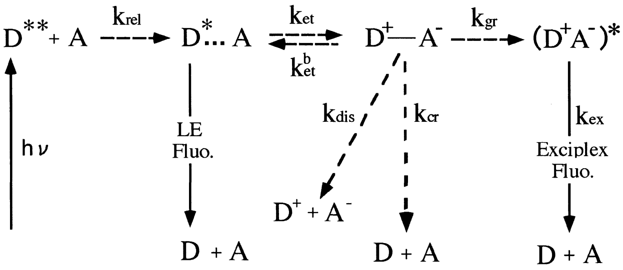

Scheme 1.

Here, D and A corresponds to ECZ and DMTP, respectively, in a mixture of ECZ and DMTP. D^{**} is the photoexcited state of ECZ, and k_{rel} is the rate constant of relaxation from D^{**} to D^{*}, following which a bimolecular encounter, $D^{*}\cdots A$, is formed. This relaxation process includes both the internal conversion to the lowest excited state of S_1 and the excitation energy migration among different molecules of ECZ. $D^{*}\cdots A$ may have a suitable conformation for the electron transfer from D^{*} to A. ECZ and DMTP do not form a complex in the ground state, and the excited state charge transfer occurs only upon bimolecular encounter of an excited molecule and a quencher. The electron transfer process competes with the radiative process from D^{*} which gives the LE(ECZ) fluorescence. D^{+}–A^{-} shows a radical–ion pair state produced by the electron transfer, whose rate is given by k_{et}. $(D^{+}A^{-})^{*}$ represents the fluorescent exciplex, and k_{gr} is the rate constant of the exciplex formation from the radical-ion pair state. k_{cr} and k_{ex} represent the rate constants for the charge recombination of the radical–ion pair and the decay rate constant of the fluorescent exciplex, respectively. Actually, a back-electron transfer which produces the excited state of ECZ need not be considered; $k_{et}{}^{b} = 0$ in a mixture of ECZ and DMTP. The relaxation processes between D^{+}–A^{-} and $(D^{+}A^{-})^{*}$ are presented as irreversible in Reaction Scheme 1, but it is not yet clear whether or not the process is irreversible.

A field-assisted dissociation to free carriers with a rate constant of k_{dis} must be considered, if a charge can move from a molecule to a neighboring molecule in the presence of ***F***. This dissociation, which will be important at high concentrations of donor or acceptor, is related to the field-induced quenching of the exciplex fluorescence (see Fig. 6) and is related to the photocurrent generation. If a hole can transport among ECZ molecules, the efficiencies both of the photocurrent generation and of the field-induced quenching of the exciplex fluorescence are expected to become higher with increasing the ECZ concentration. If an electron can transport among DMTP molecules, it is also expected that both efficiencies will become higher with increasing the DMTP concentration. The fact that exciplex fluorescence is quenched by ***F*** only when the ECZ concentration is high shows that only holes can move among ECZ molecules and that electrons cannot move among DMTP molecules.

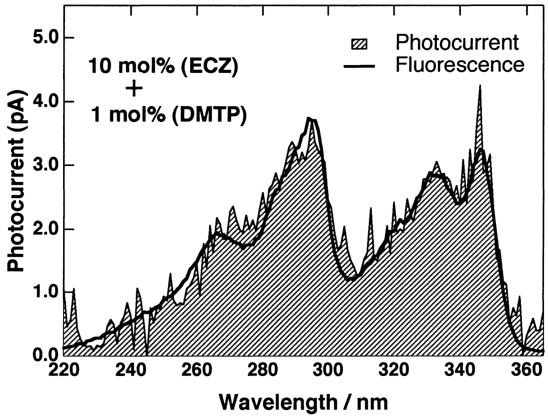

Fig. 7. Photocurrent excitation spectrum and fluorescence excitation spectrum (solid line) of a mixture of ECZ (10.0 mol%) and DMTP (1.0 mol%).

In order to verify the hypothesis that the efficiencies of hole transport and of electron transport are very different from each other, photocurrent generation has been examined in relation to the field effect on exciplex fluorescence. In fact, a photocurrent was detected when the ECZ concentration is as high as 5 or 10 mol%.[19] The photocurrent excitation spectrum observed for a mixture of 10 mol% ECZ and 1 mol% DMTP doped in PMMA is essentially the same in shape as the fluorescence excitation spectra (see Fig. 7), indicating that the detected current is generated following photoexcitation of ECZ. Field-induced quenching of the exciplex fluorescence is much larger at 10 mol% of ECZ than that at 5 mol%. The detected photocurrent is also larger at 10 mol% than at 5 mol%. Thus, the field-induced quenching of the exciplex fluorescence is well correlated to the photocurrent generation, demonstrating that the measurements of the E-F spectra are very useful to examine the mobility of electrons or holes in solid films.

Electric field effects on fluorescence of other pairs of D and A doped separately in a polymer film are briefly described.[64] E-F spectra of a mixture of phenanthrene (PHE) and *N*-methylphthalimide (NMPI) doped in a PMMA polymer film at different concentrations are shown in Fig. 8. At low concentrations, emission is dominated by the LE fluorescence of PHE, and the E-F spectrum is given by the first derivative of the fluorescence spectrum, indicating that only the Stark shift is induced because of a nonzero value of $\Delta\overline{\alpha}$ between the fluorescent state and the ground state. As the concentration increases, broad exciplex fluorescence appears in a longer wavelength region, indicating that PIET occurs from the excited state of PHE to NMPI. Under such conditions, LE fluorescence of PHE is quenched by ***F***. Thus, the rate of PIET is increased in the presence of ***F***, in agreement with the pair of ECZ and DMTP. The magnitude of the quenching becomes larger with

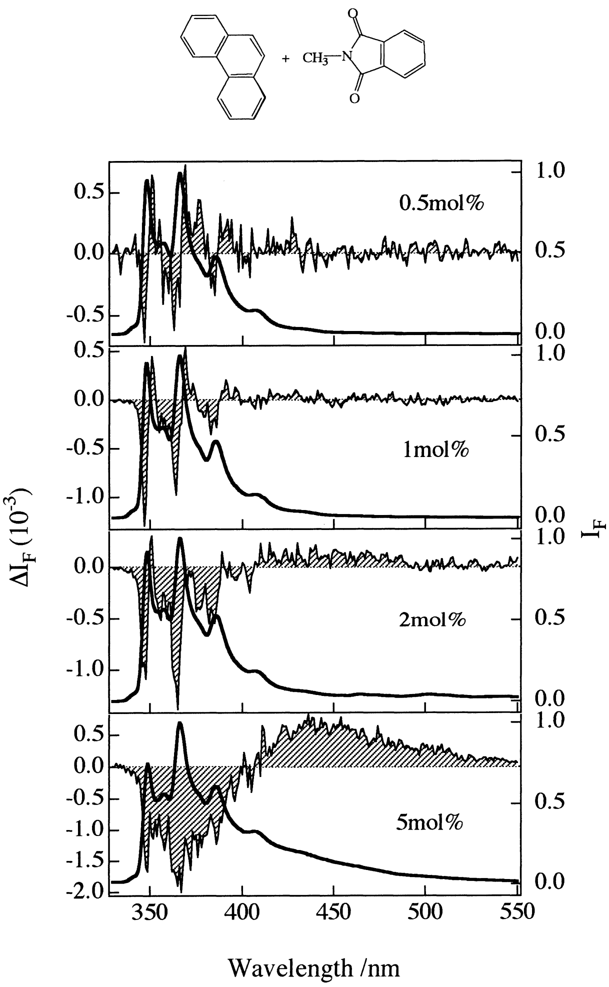

Fig. 8. Fluorescence spectra (solid film) and E-F spectra of a mixture of phenanthrene (PHE) and *N*-methylphthalimide (NMPI) doped in a PMMA film at different concentrations. The concentrations of PHE and NMPI are the same in every case. Excitation wavelength was in the region of 295.0–295.5 nm. The maximum fluorescence intensity is normalized to unity in every case. Applied field strength was 1.0 MV cm^{-1}.

increasing the concentration, indicating that both the rate and its field-induced change of PIET from the excited state of PHE to NMPI, i.e., k_{et} and Δk_{et}, increase with shortening the D–A distance. In contrast with the LE fluorescence of PHE, exciplex fluorescence increases in the presence of $\boldsymbol{F}$, probably as a result of field-induced enhancement of PIET. The absence of the field-induced quenching of the exciplex fluorescence implies that both hole mobility and electron mobility are very inefficient among PHE or NMPI molecules, respectively. In a mixture of PHE and NMPI, therefore, only k_{et} is considered to be enhanced by $\boldsymbol{F}$ in Reaction of Scheme 1. A marked difference in efficiency of the field-induced quenching of the exciplex fluorescence between a pair of ECZ and DMTP and a pair of PHE and NMPI shows that both hole mobility and electron mobility are definitely dependent on the molecule employed as a donor or acceptor.

The Stark shift which gives the E-F spectrum given by the first derivative of the fluorescence spectrum is observed both for the LE fluorescence and for the exciplex fluorescence, indicating that $\Delta\bar{\alpha}$ is significant and that $\Delta\mu$ is negligible. Based on the analysis with Eq. 5, $\Delta\bar{\alpha}$ of the LE fluorescence of ECZ is estimated to be ~100 in units of $4\pi\varepsilon_0$ Å^3, while $\Delta\bar{\alpha}$ of the fluorescent exciplex is estimated to be ~1800 in units of $4\pi\varepsilon_0$ Å^3 in a mixture of ECZ and DMTP.[54] Similarly, $\Delta\bar{\alpha}$ is estimated to be ~13 and 140 in units of $4\pi\varepsilon_0$ Å^3 for the LE fluorescence of PHE and exciplex fluorescence, respectively, in a mixture of PHE and NMPI.[64] The magnitude of $\Delta\bar{\alpha}$ of fluorescent exciplex is larger than that of the LE fluorescent state by more than one order-of-magnitude in both D–A pairs.

b) Linked Compounds of Donor and Acceptor. Methylene-linked compounds of donor (D) and acceptor (A) also show a remarkable electric field effect on fluorescence. However, some effects are very different from the ones observed in a mixture of D and A separately doped in a solid film, implying that the methylene chain plays a significant role both in photoexcitation dynamics and in its field dependence. It is confirmed in linked compounds that electron transfer, back-electron transfer, charge recombination and dissociation of radical ion-pair are influenced by $\boldsymbol{F}$, and Reaction Scheme 1 is also applicable to interpret the field effects on excitation dynamics.[64–70]

At first, electric field dependence of PIET in linked compounds of carbazole–$(CH_2)_n$–(terephtalic acid methyl ester), denoted by CZ–(*n*)–TAM or D–(*n*)–A, is described. E-F spectra of linked compounds with short and long methylene chains, respectively, i.e., CZ–(3)–TAM and CZ–(20)–TAM, doped in PMMA are shown in Fig. 9, together with the fluorescence spectra. At low concentrations, fluorescence is dominated by the LE fluorescence of carbazole chromophore (CZ), and the exciplex fluorescence is very weak, implying that the formation of intramolecular exciplex is very inefficient in PMMA films even in linked compounds. With increasing the concentration, exciplex fluorescence becomes stronger, indicating that exciplex resulting from the intermolecular processes appears, probably because D and A belonging to different molecules can approach closely and have a suitable conformation for an exciplex formation.

As shown in Fig. 9, LE fluorescence of CZ is always quenched in the presence of $\boldsymbol{F}$, and the magnitude of the quenching becomes larger with increasing concentration. These effects are very similar to the ones observed for a mixture of ECZ and DMTP doped in PMMA. The field-induced quenching is attributed to the enhancement of the rate constant of electron transfer (k_{et}), as in the case of a mixture of ECZ and DMTP. The concentration dependence of the quenching in linked compounds is similar to that for a mixture of ECZ and DMTP, which results from the intermolecular D–A distance dependence of both k_{et} and its field-induced change (Δk_{et}).

Based on the measurements of the field-induced change in fluorescence decay profile, the lifetime shortening of the LE fluorescence in the presence of $\boldsymbol{F}$ was directly observed, confirming that the field-induced quenching of the LE fluorescence results from Δk_{et}.[68] At high concentrations, intermolecular exciplex composed of the excited state of CZ and TAM is dominant, and exciplex fluorescence is quenched in the presence of $\boldsymbol{F}$. The field-induced quenching of the exciplex fluo-

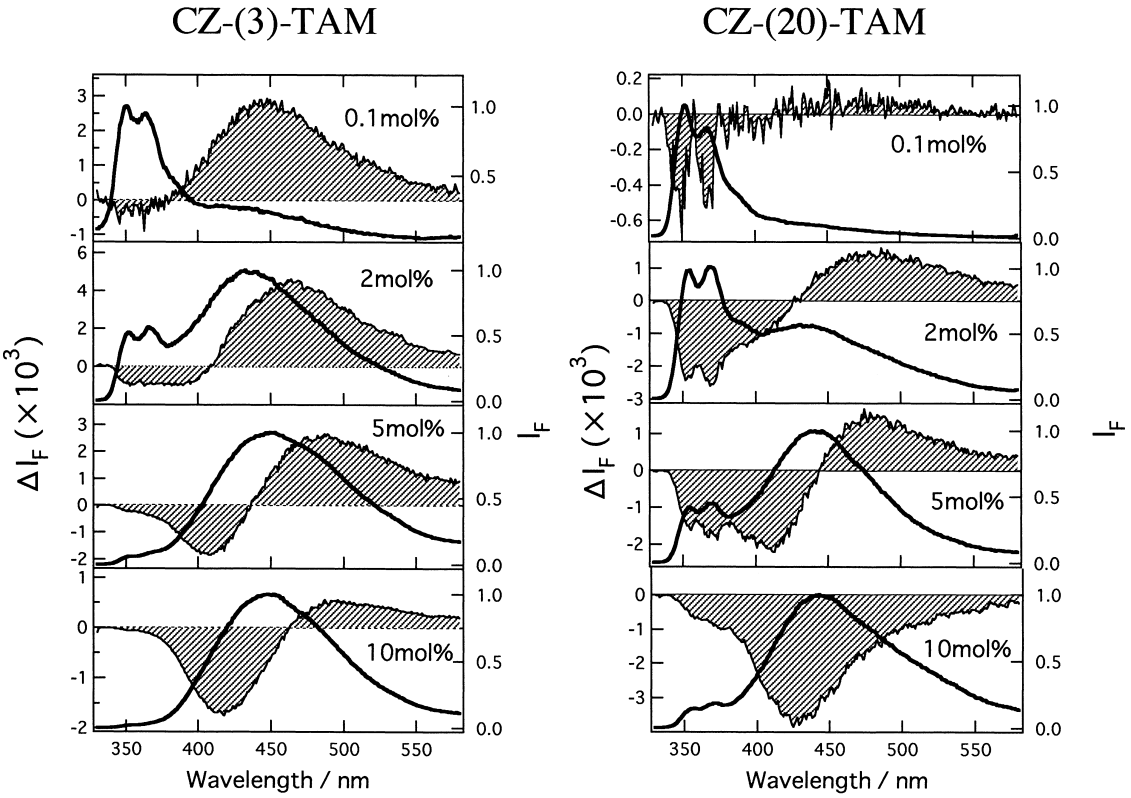

Fig. 9. Fluorescence spectra (solid line) and E-F spectra of CZ-(3)-TAM (left) and CZ-(20)-TAM (right) doped in a PMMA film at different concentrations. Applied field strength was 0.5 MV cm^{-1}. Excitation wavelength was in the region of 294.0–295.0 nm, and the maximum fluorescence intensity is normalized to unity.

rescence is attributed to a field-assisted dissociation of radical-ion pairs to free carriers; k_{dis} in Reaction of Scheme 1 increases in the presence of ***F***.[66] As already mentioned, hole mobility is very efficient among ECZ molecules, whereas an electron does not move among DMTP molecules. Then, the efficient quenching of the exciplex fluorescence in CZ-(*n*)-TAM probably results from an efficient mobility of holes among CZ chromophores.

At low or medium concentrations, exciplex fluorescence is enhanced in the presence of ***F***, and a remarkable chain length dependence is observed. As the chain length becomes shorter, the magnitude of the field-induced enhancement of the exciplex fluorescence becomes larger, as shown in Fig. 10. Especially, a marked chain length dependence is observed with *n* less than 5 in CZ-(*n*)-TAM. When the chain length becomes longer than $n = 5$, the magnitude of the enhancement looks limited.

Remarkable field-induced enhancement of the exciplex fluorescence can be also interpreted in terms of Reaction Scheme 1, by assuming that the radical ion-pair shows a charge recombination at zero field. D^+ and A^- of an ion pair which are bound to each other have a probability of recombining because of the Coulomb potential. When a charge recombination occurs in the ion-pair state, exciplex fluorescence is quenched because of the decrease in exciplex formation efficiency. The charge recombination may be enhanced by ***F*** when the field is antiparallel to the dipole moment of D^+–A^-. In other cases, however, recombination processes are presumably inhibited by ***F***. Then, the exciplex fluorescence is expected to be enhanced in the presence of ***F***. Field-induced inhibition of the charge recombination, which leads to a fluorescence enhancement, competes with the field-assisted dissociation, i.e., carrier generation, which leads to a fluorescence quenching. The former effect is important only at low concentrations. The latter effect becomes more important with increasing concentration. Actually, the magnitude of the field-induced enhancement decreases with increasing the concentration. It is also noted that the E-F spectra could be simulated by a linear combination between the fluorescence spectrum and its first derivative spectrum, indicating that the Stark effects induced by a nonzero value of $\Delta\alpha$ also exists besides the field-induced change in fluorescence quantum yield, which is similar to the above-mentioned mixtures of D and A.

A methylene chain plays a significant role in the enhancement of the exciplex fluorescence. In order to interpret the chain length dependence at medium concentrations, e.g., 1 mol%, both intra- and intermolecular processes must be considered. Here, three D–(*n*)–A molecules, denoted by *i*, *j* and *k*, respectively, are considered with the following arrangement: D_i–(*n*)–($A_i^-\cdots D_j^+$)–(*n*)–($A_j^-\cdots D_k^+$)–(*n*)–A_k, where we assume the electron transfer from donors of molecules *j* and *k* to acceptors of molecules *i* and *j*, respectively, and the ion-pair state which leads to the fluorescent exciplex state is formed between molecules *i* and *j* and between *j* and *k*. If the intramolecular charge recombination occurs in this arrangement, i.e., within *j* molecule, both ion pairs disappear and exciplex fluo-

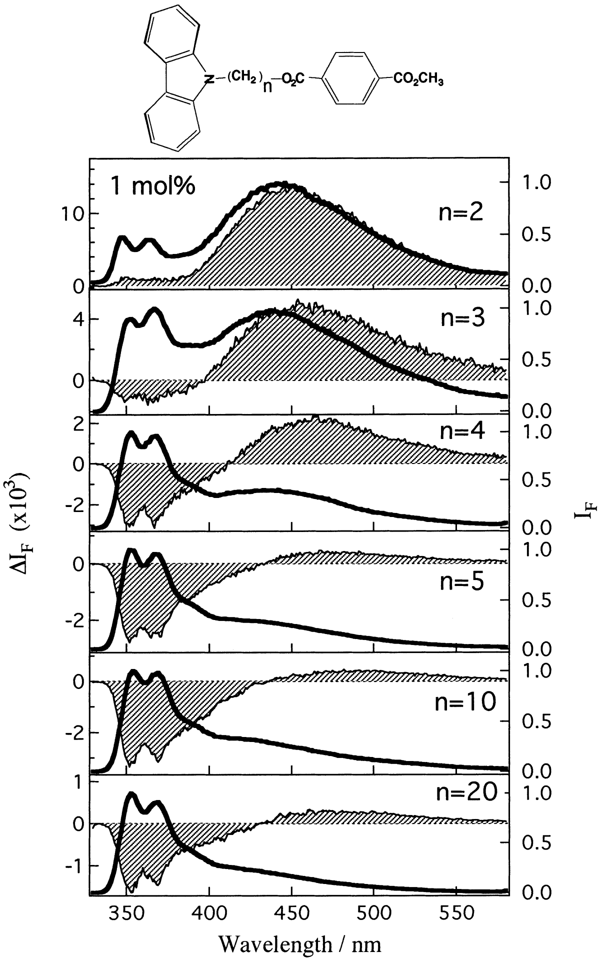

Fig. 10. E-F spectra of CZ-(*n*)-TAM with *n* from 2 to 20 doped in a PMMA film at 1.0 mol%, together with the fluorescence spectra (solid line). The maximum fluorescence intensity is normalized to unity in every case. Applied field strength was 0.6 MV cm^{-1}.

rescence is quenched. The intramolecular charge recombination results from the Coulomb interaction, and so the efficiency of the recombination may become higher as the D–A distance becomes shorter. Then, such an intramolecular recombination, which leads to a quenching of intermolecular exciplex fluorescence, is expected to occur more efficiently as the chain length becomes smaller. If the intramolecular charge recombination is thoroughly prevented by ***F***, exciplex fluorescence increases by the amount of intensity quenched by the recombination. Thus, fluorescence enhancement observed at medium concentrations is attributed dominantly to the field-induced inhibition of the intramolecular charge recombination through a bond, which probably occurs following the intermolecular PIET. The methylene chain is not always straight. A methylene chain in CZ–(20)–TAM may be like a random coil. Then, the D–A distance in each molecule of CZ–(20)–TAM may be not so different from that of CZ–(3)–TAM. If a charge recombination occurs through a space, not only through a bond, the enhancement might be independent of the chain length. Therefore, the monotonic chain length dependence suggests that the charge recombination through a bond occurs very efficiently.

LE fluorescence of CZ–(*n*)–TAM is quenched in the presence of ***F***, as mentioned above. This is true when *n* is larger than 3. When the methylene chain is very short, i.e., in CZ–(2)–TAM, LE fluorescence is slightly enhanced by ***F*** (see Fig. 10).[69] The enhancement of the LE fluorescence is interpreted by assuming an efficient back-electron transfer in Reaction Scheme 1. If the population of the radical–ion pair is increased by the field-induced inhibition of the charge recombination through a bond, the efficiency of the back-electron transfer is increased. As a result, LE fluorescence as well as exciplex fluorescence is enhanced in the presence of ***F***. Thus, the efficiency of the back-electron transfer is considered to be also influenced by ***F***.

Other linked compounds of D and A also show significant electric field effects on fluorescence, which can be interpreted in terms of Reaction Scheme 1. E-F spectra are shown in Fig. 11 for PY-(3)-PI and PY-(3)-DMA, where PY, PI and DMA represent the chromophores of pyrene, phthalimide and *N*,*N*-dimethylaniline, respectively, and in Fig. 12 for PH–(*n*)–PI, where PH and PI represent phenanthrene and phthalimide chromophores, respectively. Both in PY–(3)–PI and in PY–(3)–DMA, where PY acts as a donor in the former and as an acceptor in the latter, LE fluorescence of PY is significantly quenched in the presence of ***F*** even at very low concentrations. Further, the magnitude of the quenching increases monotonically with increasing the concentration, indicating that both intra- and intermolecular processes of PIET are enhanced in the presence of ***F***. Efficient back-electron transfer need not be considered in the two compounds, and the quenching of the exciplex fluorescence at high concentrations suggests a photocarrier generation. Electron mobility among PI chromophores is very inefficient, as mentioned in a mixture of PHE and NMPI. Hole mobility among DMA chromophores is not so efficient either.[70] Accordingly, mobilities both of hole and of electron among pyrene chromophores are known to be very efficient in solid films.

As shown in Fig. 12, E-F spectrum of PH–(12)–PI at low concentrations is very similar to the first derivative of the fluorescence spectrum, indicating that only the Stark shift is observed and that the intramolecular process is negligible both in the absence and in the presence of ***F***. With increasing concentration, some exciplex fluorescence resulting from PIEI between PHE and PI chromophors appears, and the LE fluorescence is quenched in the presence of ***F***. Thus, intermolecular PIET is enhanced in the presence of ***F***. When the chain length becomes shorter, on the other hand, E-F spectra at low concentrations are quite similar in shape to the fluorescence spectrum, and the integrated intensity is anomalously positive, indicating that LE fluorescence is enhanced in the presence of ***F***. At high concentrations, exciplex fluorescence appears as a result of intermolecular PIET from the excited PH to PI chromophore, and the field-induced quenching is observed for the LE fluorescence. As the concentration increases, the magnitude of the field-induced enhancement of the LE fluorescence becomes smaller monotonically, indicating that LE fluorescence is enhanced and quenched as a result of the field effect on intramolecular processes and as a result of the field effect on intermolecular processes, respectively. Thus, it seems that the electric field effects on intramolecular and intermolecular processes

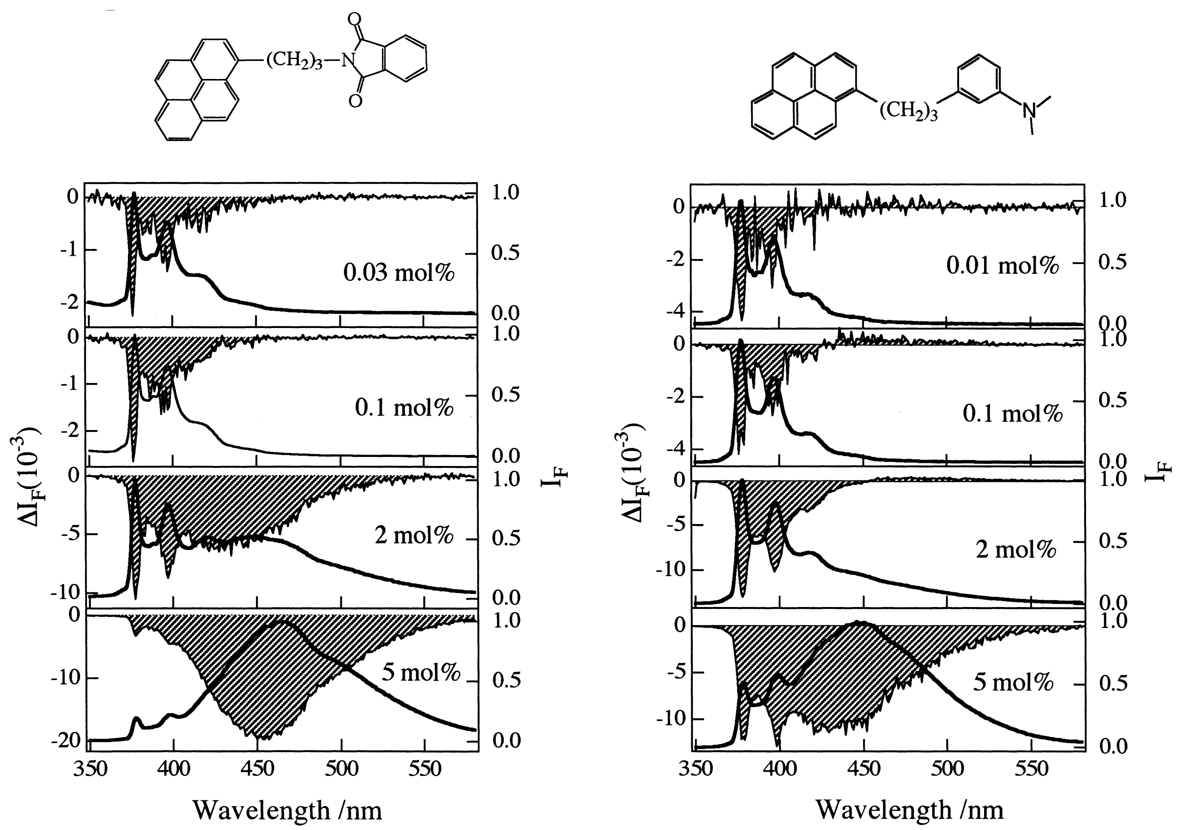

Fig. 11. E-F spectra of PY-(3)-PI (left) and PY-(3)-DMA (right) doped in a PMMA film at different concentrations, together with the fluorescence spectra (solid line). Applied field strength was 1.0 MV cm^{-1}. The maximum fluorescence intensity is normalized to unity in every case. Excitation wavelength was in the region of 318.5–321.0 nm.

are completely opposite.

These results may be also interpreted in terms of Reaction Scheme 1. D and A correspond to PH and PI chromophores, respectively. It is assumed that a back-electron transfer occurs efficiently in PH–(3)–PI from D^+–A^- to $D^*\cdots A$ with a rate constant of k_{et}^{b}. As far as the same pairs of D and A chromophores are employed, it would be unlikely that the opposite field effects on the electron transfer are induced between intramolecular and intermolecular processes. It seems very likely that k_{et} in scheme I increases in the presence of $\boldsymbol{F}$ for both intra- and intermolecular processes, though the magnitudes of the increase may be different from each other. Then, it is considered that PH-(3)-PI shows a reversible intramolecular PIET and that the efficiency of the back-electron transfer, which produces the fluorescent state of PH, becomes larger in the presence of $\boldsymbol{F}$. The increase of the efficiency in back-electron transfer may result from the field-induced inhibition of the charge recombination through a short methylene chain, i.e., k_{cr} in Reaction Scheme 1 decreases in the presence of $\boldsymbol{F}$, as in the case of CZ–(*n*)–TAM.

As mentioned above, the field effects on the initial step of electron transfer in solid films seem to be the same both for the D and A separately doped system and for the linked system; the rate is enhanced in the presence of $\boldsymbol{F}$. However, a remarkable enhancement of the LE fluorescence and of exciplex fluorescence is observed in the presence of $\boldsymbol{F}$ only for linked compounds of D and A, e.g., CZ–(2)–TAM and PH–(3)–PI. These phenomena are very sensitive to the chain length, and such peculiar behavior comes from the field effects on the charge recombination and/or back-election transfer though a bond. It should be also noted that a remarkable field-induced enhancement of fluorescence is not always observed, but depends crucially on the pair of D and A, suggesting that free energy gap for the reaction and geometrical restrictions for exciplex formation play a significant role in the field effects which are characteristic of the linked compounds.[71] These results also suggest that a linkage by a molecular chain plays an unpredictable effect both on photoexcitation dynamics and on its electric field dependence under certain conditions.

c) Vectorial Interlayer Electron Transfer. Electron donor and acceptor layers separated by a spacer layer have been prepared with a cyanine dye as a donor and viologen as an acceptor using an LB technique. A schematic illustration of the prepared layer structure is shown in Fig. 13 for D–A pairs of *N*,*N*′-dioctadecyloxacarbocyanine (OCC) and *N*,*N*′-dioctadecyl-4,4′-bipyridinium dibromide (VIO) with a spacer layer of arachidic acid (AA). Besides an AA layer, an LB monolayer film of palmitic acid, stearic acid and behenic acid was used as a spacer layer between OCC and VIO. In these systems, interlayer vectorial photoinduced electron transfer occurs from the excited state of OCC to VIO through a spacer layer. As a result, fluorescence quenching and lifetime shortening of the OCC fluorescence are observed in the presence of the VIO layer. Actually, each layer of OCC and VIO was deposited as a

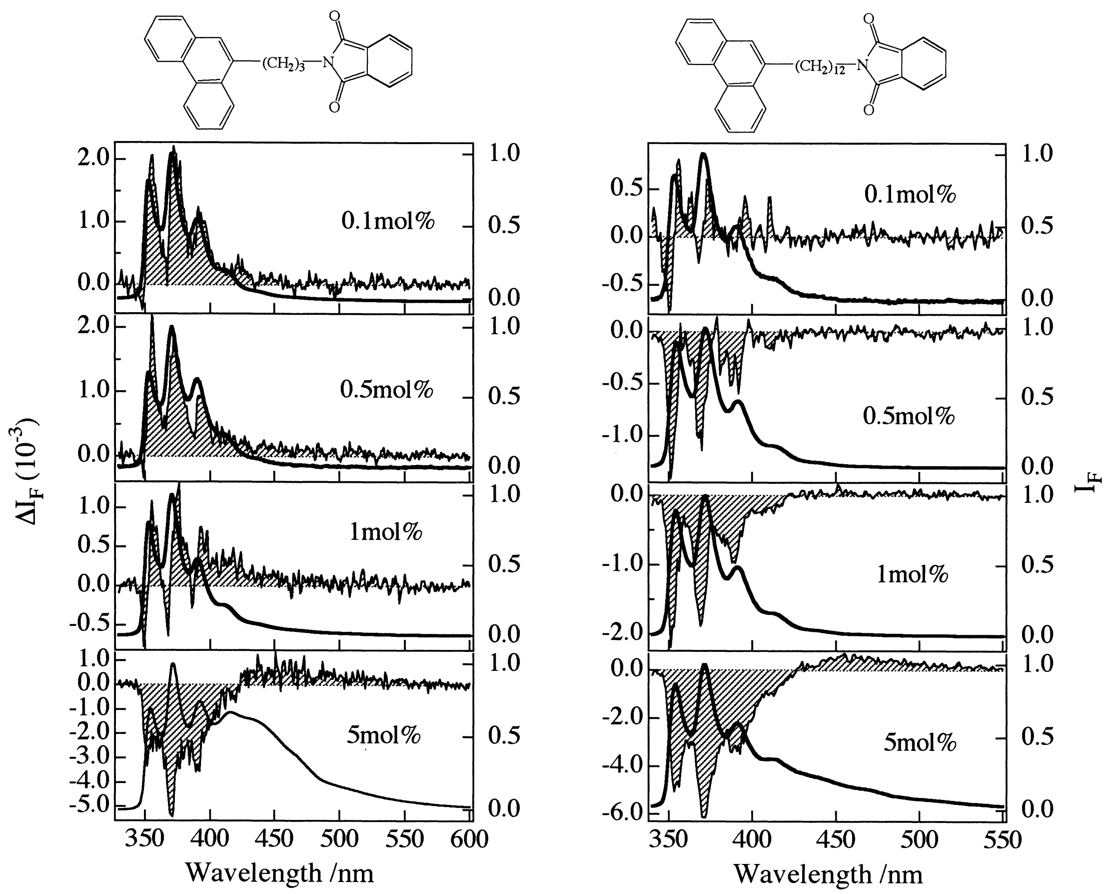

Fig. 12. E-F spectra of PH-(3)-PI (left) and PH-(12)-PI (right) doped in a PMMA film at different concentrations, together with the fluorescence spectra (solid line). Applied field strength was 1.0 MV cm^{-1}. Excitation wavelength was in the region of 298.5–301.5 nm. The maximum fluorescence intensity is normalized to unity in every case.

mixture with a fatty acid.

A mixture of AA and methyl arachidate (MA) whose ratio is 1:1 (AA/MA) was used as a matrix. Various mixing fractions of OCC to AA/MA have been employed. Two kinds of stacking multilayer films were prepared: one includes a VIO monolayer (sample(1)), and the other doesn't include a VIO monolayer (sample(2)). Sample (1) was prepared as follows: at first, seven layers of AA were deposited on the quartz substrate coated by a semi-transparent aluminum film; one mixed monolayer composed of OCC and AA/MA was deposited; one AA monolayer was deposited; one mixed monolayer composed of VIO and AA/MA was deposited; deposition of these three monolayers were repeated with a spacer of four monolayers of AA; seven layers of AA were deposited for protection; a semi-transparent aluminum film was again coated with evaporation. Aluminum films were used as electrodes. Sample (2) has the same layer structure as sample (1) except that the VIO mixed layer is replaced by an AA layer.

As the OCC fraction increases, absorption spectrum and fluorescence spectra change, indicating that molecular aggregates (probably OCC dimer) are formed at high OCC fractions.[51] Figure 14 shows fluorescence spectra and E-F spectra of samples (1) and (2) with a low OCC fraction of 0.5 mol%, where fluorescence spectra are very similar to a diluted-solution spectrum of OCC and can be regarded as the monomer fluorescence spectra of OCC. In the presence of VIO, fluorescence intensity is reduced by about 20%.[72] This quenching is attributed to the electron transfer from the fluorescent state of OCC to VIO, which occurs in competition with radiative and other nonradiative deactivation processes, as in the case of other cyanine dyes.[73–75] Fluorescence decays observed in the presence and in the absence of VIO also indicate that fluorescence of OCC is quenched by VIO as a result of electron transfer.[72] Fluorescence shows a non exponential decay even at a low concentration of 0.5 mol%, and so the average lifetime ($\bar{\tau}_F$) is defined, as mentioned previously. The $\bar{\tau}_F$ value is determined to be 1.0 and 0.8 ns in the absence and in the presence of VIO, respectively, indicating that the average rate constant of the electron transfer from photoexcited OCC to VIO at 0.5 mol% with a spacer layer of AA, denoted by k_{et}, is 2.5×10^8 s^{-1}.

The E-F spectrum of OCC in the absence of VIO, observed at the first harmonic of the modulation frequency, is very similar to the first derivative of the fluorescence spectrum, as shown in Fig. 14, indicating that the field effect on the fluorescence spectrum of the OCC monomer in the absence of VIO results from the Stark shift induced by a non-zero value of $\Delta\mu$ between the ground state and the fluorescent S$_1$ state. The E-F spectra indicate that the fluorescence spectrum shows a blue shift in the presence of $\boldsymbol{F}$ with the molecular arrangement and the field direction shown in Fig. 13.

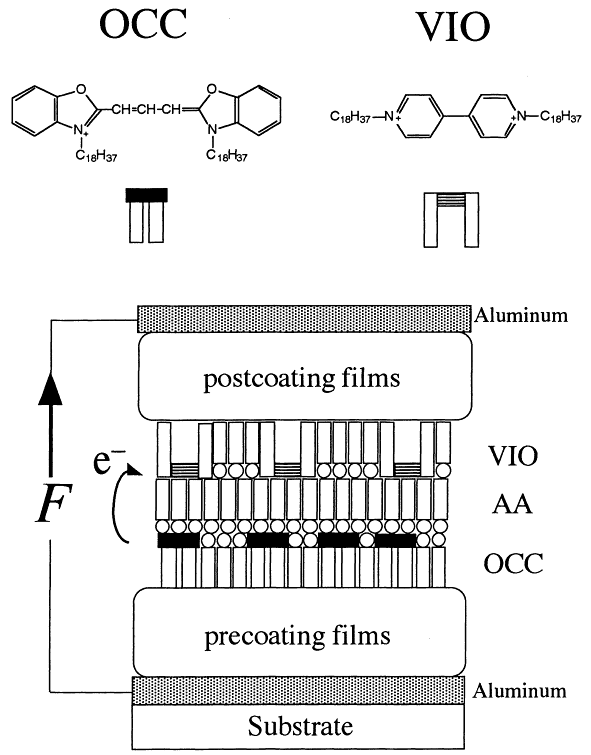

Fig. 13. Schematic illustration of LB multilayer films composed of OCC mixed monolayer and VIO mixed monolayer separated with a spacer layer of AA. The direction of the applied electric field and the direction of the electron transfer are shown by an arrow and a half arrow, respectively.

The E-F spectra of OCC observed in the presence of VIO are very different from the ones in the absence of VIO, as shown in Fig. 14. The E-F spectra in the presence of VIO are quite similar in shape to the fluorescence spectra, indicating that the fluorescence quantum yield of OCC is significantly affected by $\boldsymbol{F}$. The E-F spectra shown in Fig. 14 were obtained with the field direction shown in Fig. 13 with the excitation wavelength where ΔA is negligible. When the field direction is inverted, the spectral shape and the magnitude of the field-induced change are essentially the same, but the sign of the spectra is changed (see Fig. 15). Thus, the fluorescence quantum yield is increased by $\boldsymbol{F}$ with the field direction shown in Fig. 13, whereas the quantum yield is decreased by $\boldsymbol{F}$ with the opposite field direction.[72,76] Actually, the E-F spectra in the presence of VIO could be simulated by a combination of the fluorescence spectrum and its first derivative, i.e., both the Stark shift induced by a change in $\boldsymbol{\mu}$ between the fluorescent state and the ground state and the field effect on the fluorescence quantum yield are induced in the presence of VIO. The ratio of $\Delta\Phi_F^{VIO}/\Phi_F^{VIO}$ could be evaluated from the fluorescence intensity and its field-induced change. Here, Φ_F^{VIO} and $\Delta\Phi_F^{VIO}$ represent the fluorescence quantum yield of OCC and its field-induced change in the presence of VIO, respectively. The results show that $\Delta\Phi_F^{VIO}/\Phi_F^{VIO}$ is linearly proportional to the applied field strength and is given by 1.7×10^{-9} $\boldsymbol{F}$ in units of V cm^{-1} for $\boldsymbol{F}$.

The field effect of $\Delta\Phi_F^{VIO}$ can be interpreted in terms of the field effect on the rate of electron transfer which occurs from the photoexcited OCC to VIO. With a simple kinetic scheme, Φ_F^{VIO} and $\Phi_F^{VIO} + \Delta\Phi_F^{VIO}$ can be expressed by $k_r/(k_r + k_{nr} + k_{et})$ and $k_r/(k_r + k_{nr} + k_{et} + \Delta k_{et})$, respectively. Here, k_r, k_{nr}, k_{et}, and Δk_{et} represent the radiative rate constant, nonradiative decay rate constant except for electron transfer, electron transfer rate constant and its field-induced change, respectively. Then, Δk_{et} is given by Eq. 6. By employing the above-mentioned value of $\bar{\tau}_F$ in the presence of VIO, i.e., $\bar{\tau}_F^{VIO}$ (0.8 ns), Δk_{et} is de-

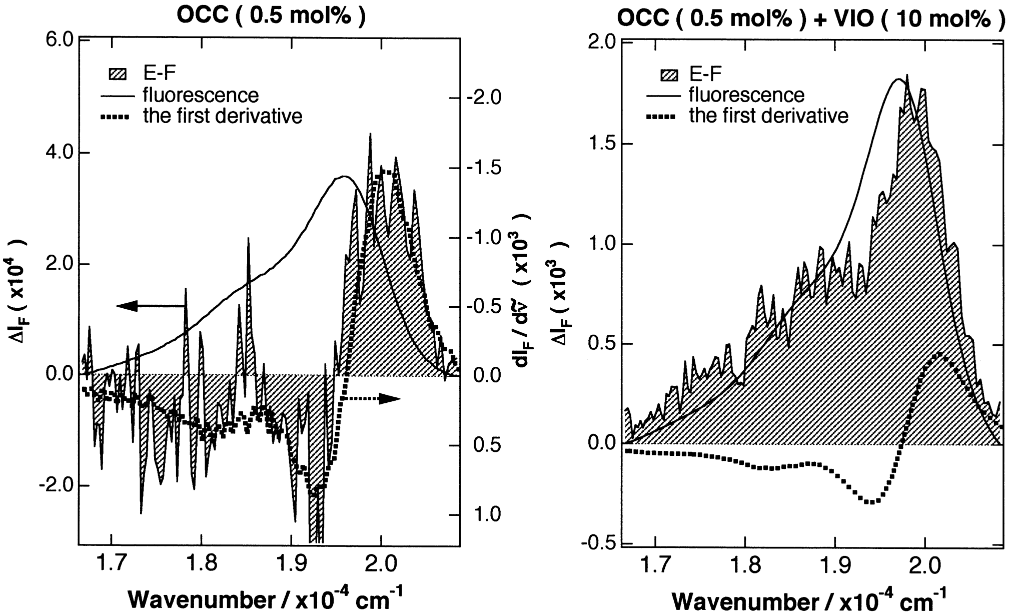

Fig. 14. Fluorescence spectra (solid line) and E-F spectra of OCC with a field strength of 1.0 MV cm^{-1} in LB films. The spectra in the right were obtained in the presence of VIO, while the spectra in the left were obtained in the absence of VIO. The dotted line shows the first derivative of the fluorescence spectrum. Excitation wavelength was 430.0 nm.

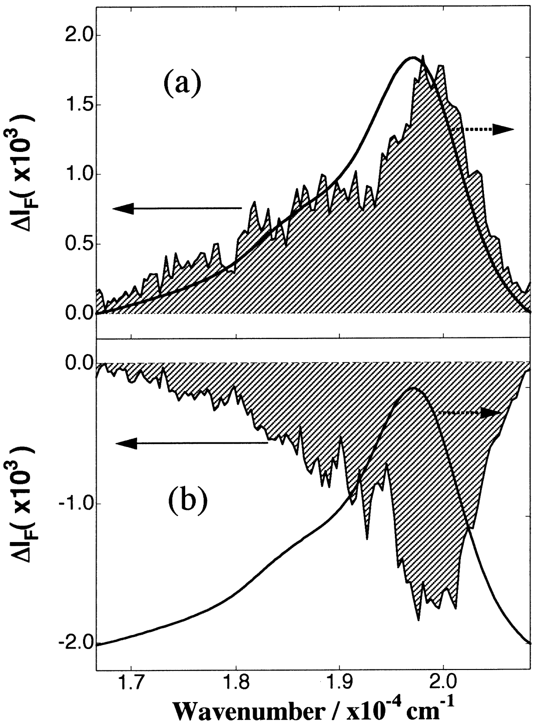

Fig. 15. E-F spectra observed with a field direction shown in Fig. 13(a) and with the opposite field direction (b), together with the fluorescence spectra (solid line). Field strength was 1.0 MV cm^{-1}. The maximum fluorescence intensity is normalized to unity.

termined to be $-2.1\,\boldsymbol{F}$ in units of s^{-1} at 0.5 mol% using units of V cm^{-1} for $\boldsymbol{F}$. The negative value indicates that the electron transfer becomes slower as the field becomes stronger with the same direction as in Fig. 13. Note that the electron transfer is enhanced in the presence of $\boldsymbol{F}$ with the opposite direction and that the sign of the above-mentioned Δk_{et} changes.

The electron transfer rate depends on various parameters: the free energy gap between the initial and final states; the magnitude of the electronic coupling between D and A, which depends on the mutual distance and orientation; the overall reorganization energy involving both the external and internal reorganization. On photoinduced vectorial electron transfer through a fatty acid monolayer in the molecular architecture of LB assemblies, D–A distance dependence of the fluorescence quenching suggests that electron tunneling through a potential barrier of a fatty acid occurs from the initial state.[73–75,77] In such a case, k_{et} may be proportional to K which is expressed as follows:

$$K = K_0 \exp(-\beta d),\ \beta = 2(2m\phi)^{1/2}/\hbar \tag{10}$$

Here m is the electron mass, $\hbar$ is Planck's constant divided by 2π, ϕ is a height of barrier represented by the fatty acid spacer, and d is the D–A distance. External electric field may play a role to change a barrier height of tunneling. When an external electric field is applied with a direction in Fig. 13, the barrier height may become higher, while the barrier may become lower in the opposite direction. Then, ϕ may be replaced by $\phi_0 + \phi'\boldsymbol{F}$ in the presence of $\boldsymbol{F}$, where ϕ_0 is the height at zero field and ϕ' is the first derivative of the potential barrier with respect to the field strength. By using Eq. 10, $\Delta k_{\mathrm{et}}(\boldsymbol{F})$ divided by $k_{\mathrm{et}}(\boldsymbol{F} = 0)$ may be approximately given by

$$\Delta k_{\mathrm{et}}(\boldsymbol{F})/k_{\mathrm{et}}(\boldsymbol{F} = 0) = [2md\hbar^{-1}(2m\phi_0)^{-1/2}(\phi'\boldsymbol{F})] \tag{11}$$

In the present D–A system, k_{et} and Δk_{et} were determined to be 2.5×10^8 s^{-1} and $-2.1\,\boldsymbol{F}$ s^{-1}, respectively; $\Delta k_{\mathrm{et}}/k_{\mathrm{et}}$ is $-8.4 \times 10^{-9}\,\boldsymbol{F}$, where $\boldsymbol{F}$ is written in units of V cm^{-1}. It is worth mentioning that the negative sign shows the de-enhancement of the electron transfer rate with the field direction in Fig. 13. When 0.7 eV is employed as ϕ_0,[78] the above value of $\Delta k_{\mathrm{et}}/k_{\mathrm{et}}$ can be reproduced with ϕ' of 3.2×10^{-9} eV(V/cm)$^{-1}$.

E-F spectra with various fatty acid spacers were observed at 2 mol% of OCC. At this fraction, some fluorescence emitted from an aggregate of OCC (probably dimer) with a peak at ~16500 cm^{-1} exists, but most fluorescence is emitted from the OCC monomer, as in the case of the 0.5 mol% mixed monolayers. In the presence of VIO, fluorescence quenching is observed as a result of PIET from the excited state of OCC to VIO, irrespective of $\boldsymbol{F}$. The magnitude of the quenching becomes larger with shortening the spacer distance, and the electron transfer rate is proportional to the exponential function of the spacer distance, i.e., D–A distance. A similar dependence of the fluorescence quenching on the D–A distance has been reported in other LB film systems which show PIET.[73–75,79]

The magnitude of the quenching of the OCC fluorescence, which occurs in the presence of the VIO mixed layer, significantly depends on the spacer distance, while the magnitudes of the field-induced change in fluorescence intensity relative to the total fluorescence intensity are roughly the same. The magnitudes both of k_{et} and of Δk_{et} were similarly estimated at 2 mol% of OCC for different spacer layers.[80] The evaluated values of $\Delta k_{\mathrm{et}}/k_{\mathrm{et}}$ give a straight line as a function of the spacer distance, in agreement with the expectation. From the slope of $\Delta k_{\mathrm{et}}/k_{\mathrm{et}}$, i.e., 3.4×10^{-4} Å^{-1}, ϕ' is evaluated to be 2.9×10^{-10} eV(V cm^{-1})$^{-1}$, i.e., the barrier height increase or decreases, depending on the field direction relative to the direction of the electron transfer. Note that the barrier height increases, e.g., by 0.29 meV in the presence of 1.0 MV cm^{-1} with the applied field direction shown in Fig. 13. By using the fluorescence lifetime of the OCC monomer in the absence of VIO, i.e., $\tau_F{}^0 = 1.0$ ns,[72] k_{et} as well as Δk_{et} could be estimated for each spacer. Plots of k_{et} and $|\Delta k_{\mathrm{et}}|$ are shown in Fig. 16, as a function of the spacer distance. It is clear that both k_{et} and $|\Delta k_{\mathrm{et}}|$ increase monotonically with shortening the D–A distance.

It is concluded that the electron tunneling from OCC monomer to VIO through a fatty acid monolayer is influenced by $\boldsymbol{F}$ and that the barrier height for the tunneling becomes higher and lower, depending on the field direction. It was shown that the magnitude not only of the electron transfer rate but also of its field-induced change becomes larger with shortening the D–A distance.[80] This distance dependence of k_{et} and Δk_{et} is very similar to that observed in random distribution system (cf. Figs. 5 and 16).

If the OCC fraction in mixed LB films is increased, OCC dimer is formed. The excitation dynamics of dimer is different from that of the monomer.[51] Then, field effects on excitation dynamics of OCC dimer both in the absence and in the pres-

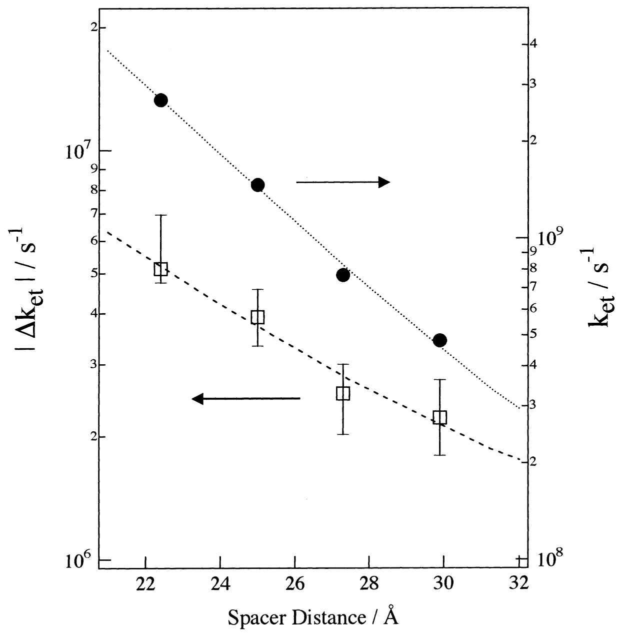

Fig. 16. Spacer distance dependence of k_{et} (●) and $|\Delta k_{\mathrm{et}}|$ (□) for interlayer PIET from OCC to VIO through a fatty acid. Applied field strength was 1.0 MV cm^{-1}.

ence of the VIO layer are briefly discussed. The fluorescence spectrum with an OCC fraction of 20 mol% is a mixture of the monomer spectrum and the dimer spectrum. The E-F spectrum of the dimer in the absence of VIO observed at the first harmonic of the modulation frequency is quite similar in shape to the dimer fluorescence spectrum, indicating that the rate of excitation dynamics of OCC dimer is enhanced by ***F*** with the field direction given in Fig. 13 even in the absence of VIO. When the field direction was inverted, the spectral shape and the magnitude of the field-induced change in fluorescence intensity were essentially the same, but the sign changed. Thus, the excitation dynamics of the dimer, which is affected by ***F*** even in the absence of VIO, is regarded as a vectorial process along the normal to the surface.

The E-F spectrum with an OCC fraction of 20 mol% in the presence of VIO is rather similar in shape to the first derivative of the fluorescence spectrum, indicating that the field-induced quenching of dimer fluorescence, which occurs in the absence of VIO with the field direction given in Fig. 13, is cancelled by the presence of VIO. As in the case of monomer, therefore, the initial step of PIET from OCC dimer to VIO is regarded as reduced by ***F*** with the field direction given in Fig. 13.[76,81] Similar field dependence was also found for interlayer electron transfer from the excited state of *N,N′*-dioctadecylthiacyanine perchlorate to VIO.[82]

2. Excimer Formation. Excimer formation process of pyrene is also influenced by ***F*** in a polymer film, indicating that the production of the radical-ion pair having a large electric dipole moment is not always necessary to induce an efficient electric field effect on photochemical processes.[83] At low concentrations of pyrene in a film, fluorescence is dominated by the sharp structured LE fluorescence emitted from the locally excited state of S_1, and the E-F spectra are essentially the same as the first derivatives of the fluorescence spectra, as shown in Fig. 2. Thus, the electric field effect on LE fluorescence at low concentrations results from the so-called Stark shifts caused by a nonzero value of $\Delta\bar{\alpha}$ between the ground state and the excited state.[50] As the concentration increases, a broad excimer fluorescence with a peak at ~470 nm appears besides the LE fluorescence (see Fig. 17). Hereafter, the excimer fluorescence with a peak at ~470 nm is referred as the first excimer fluorescence, which probably corresponds to a sandwich-type conformation.

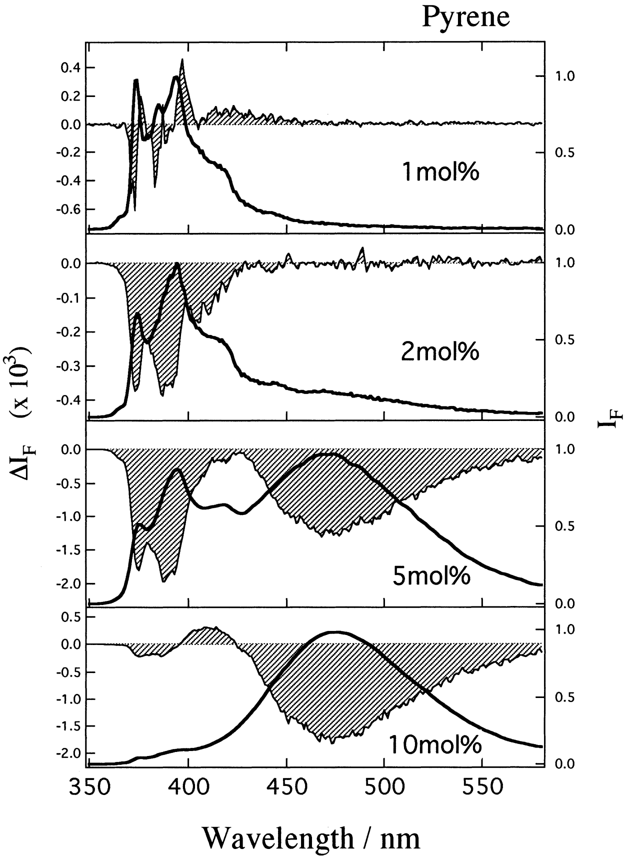

Fig. 17. E-F spectra of pyrene doped in a PMMA film at different concentrations, together with the fluorescence spectra (solid line). Applied field strength was 0.8 MV cm^{-1}. Maximum fluorescence intensity is normalized to unity in every case. Excitation wavelength was in the region of 322.0–322.5 nm.

Along with the appearance of the first excimer fluorescence, E-F spectra of the LE fluorescence become rather similar in shape to the LE fluorescence spectrum, indicating that the quantum yield of the LE fluorescence becomes smaller in the presence of ***F***. The magnitude of the quenching of the LE fluorescence relative to the total LE fluorescence intensity was evaluated to be 5.5×10^{-3} and 6.3×10^{-3} at 5 and 10 mol% , respectively, with a field strength of 1.0 MV cm^{-1}. Thus, the field-induced quenching of the LE fluorescence becomes more efficient with increasing concentration. Note that the field-induced quenching is regarded as zero at low concentrations, below 1 mol%.

E-F spectra at wavelengths longer than ~470 nm are very

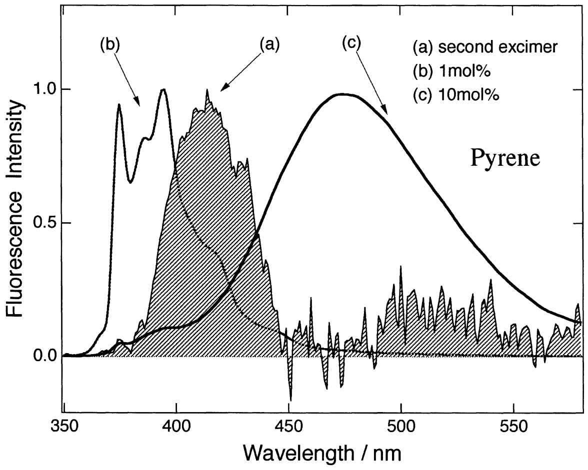

Fig. 18. Fluorescence spectrum of the second excimer of pyrene in a PMMA film (a), and the fluorescence spectra at 1.0 mol% (b) and at 10 mol% (c).

similar in shape to the excimer fluorescence spectrum, e.g., at 5 and 10 mol% (see Fig. 17), indicating that not only the LE fluorescence but also the first excimer fluorescence are quenched by ***F***. In contrast with the LE fluorescence or the first excimer fluorescence, the third fluorescence with a peak at ~415 nm is enhanced by ***F*** at high concentrations. The magnitude of the change both in enhancement and in quenching is proportional to the square of the applied field strength. The third fluorescence is very weak in the steady state fluorescence spectra, but the spectrum could be obtained using the fluorescence and E-F spectra at 10 mol%. It was assumed that fluorescence at 10 mol% is a mixture of the LE fluorescence and the first excimer fluorescence and that the E-F spectrum is given by a superposition of the LE, the first excimer and the third fluorescence spectra. The derived spectrum of the third fluorescence is shown in Fig. 18, together with the spectrum at 1.0 mol% (LE fluorescence spectrum) and the spectrum at 10 mol%, which is dominated by the first excimer fluorescence. The third fluorescence shows a broad feature with a peak at around 415 nm, and this fluorescence is attributed to a different type of excimer from the first excimer. Then, the excited species which gives the third fluorescence is called the second excimer.

A broad fluorescence other than the LE fluorescence or the first excimer fluorescence has been reported to be located in the region of 400–420 nm in a crystal,[84,85] in an LB film,[86] in a vapor deposited film of 12-(1-pyrenyl)dodecanoic acid[87] or in a neat liquid.[88] This fluorescence is assigned as a one-center or partially overlapping type of excimer, as in the case of Y-type of excimer in a perylene crystal.[89] Thus, it is very likely that the second excimer which is enhanced by ***F*** corresponds to the one-center or partially overlapping type of excimer. Fluorescence decay measurements show that the second excimer exists even in the absence of ***F*** in a PMMA polymer film and that its average lifetime is longer than that of the LE fluorescence, but shorter than that of the first excimer fluorescence.

It is likely that the electric field effects on fluorescence quantum yield result from the field-induced change in nonradiative decay rate, i.e., excimer formation rate is influenced by ***F***. The field effect on fluorescence quantum yield could be analyzed with a simple kinetic scheme. Formation rate constants of the first and the second excimers are denoted by k(I) and k(II), respectively. Their field-induced changes are represented as Δk(I) and Δk(II), respectively. By using the data of relative intensity of each component of fluorescence and the field-induced change in fluorescence quantum yield of each component, together with the average fluorescence lifetime, these rate constants were evaluated. At 10 mol%, for example, k(I) is evaluated to be 9.7×10^7 s^{-1}, while k(II) is smaller than k(I) by more than two orders of magnitude, and Δk(I) and Δk(II) were determined to be 3.6×10^5 s^{-1} and 2.7×10^5 s^{-1}, respectively, with a field strength of 1.0 MV cm^{-1}. These results show that formation rates both of the first excimer and of the second excimer are enhanced by ***F***. The formation rate of the first excimer, i.e., k(I), is much larger than that of the second excimer, i.e., k(II), whereas the magnitudes of the field-induced change in formation rate are not so different from each other. This is the reason why the opposite field dependence of the electric field effects on fluorescence intensity is observed for the first excimer and for the second excimer.

Because of the large overlap of π orbitals between adjacent two pyrene chromophores, the first excimer is much more stable than the second excimer: $k(\mathrm{I}) >> k(\mathrm{II})$. If the applied electric field induces an orbital polarization of electrons, however, the stability of the unstable excimer may be enhanced by ***F*** because of the change in orbital overlap. In fact, the second excimer was shown to be largely influenced by ***F***. Therefore, the present results imply that electric fields induce an orbital polarization even when the applied field strength is similar to the one used in the present study, i.e, in the order of MV cm^{-1}.

Similar electric field effects on fluorescence were observed for the methylene-linked compound where two pyrene chromophores are attached to the chain ends, i.e., 1,3-bis-(1-pyrenyl)propane doped in a PMMA film at high concentrations; LE fluorescence and the first excimer fluorescence are quenched by ***F***, while the second excimer fluorescence is enhanced by ***F***.[90] In comparison with bare molecules of pyrene, however, only the first excimer fluorescence is quenched extremely well by ***F***. Actually, the magnitude of the quenching is nearly proportional to the fourth power of the applied field strength in 1,3-bis-(1-pyrenyl)propane only for the first excimer fluorescence. Further, efficient electroluminescence, which is similar in shape to the first excimer fluorescence, is observed in the linked compounds, probably by a radiative recombination of the hole-electron pair through a short methylene chain. Such surprising differences of the field effects on excimer fluorescence between pyrene and methylene-linked compound may give an important guide for design of new organic materials which show efficient electroluminescence.

Summary and Future Prospect

In a mixture of electron donor (D) and acceptor (A) separately doped in a polymer film, fluorescence emitted from the locally excited state is quenched by ***F***, and the rate of intermolecular electron transfer between the excited molecule and the ground state of its counterpart is enhanced by ***F***. The field effects on the initial step of electron transfer have been discussed in terms of the field-induced change in free energy gap between reactant and product. The electronic properties of the fluorescent exciplex were examined by analyzing the Stark shift in the fluorescence spectra. The efficiency of the carrier mobility of photoinduced hole or electron in a polymer film was examined by the measurements of the E-F spectra of exciplex fluorescence.

In polymethylene-linked D and A systems doped in a PMMA polymer film, the chain length dependence is found in the electric field effects both on the LE fluorescence and on exciplex fluorescence. This dependence is interpreted by assuming that the initial step of electron transfer, charge recombination which leads to the original pair of neutral molecules, and back-electron transfer which produces the fluorescent state of the excited chromophores occur through a methylene chain. The rate or efficiency of these processes depends on the chain length. It is proposed that the charge recombination, which efficiently occurs through a bond, is inhibited by $\boldsymbol{F}$ and that the efficiency of the back-electron transfer through a bond is influenced by $\boldsymbol{F}$, and the magnitude of the field effect depends on the pair of D and A. Thus, photoexcitation dynamics of chain molecules, where two reactants are attached to chain ends, is very different in certain cases from that in unlinked systems even in solid states.

External electric field effects on vectorial interlayer PIET through a fatty acid monolayer have been examined with well-ordered molecular assemblies of LB films. Field effects on fluorescence show that the initial step of the electron transfer is enhanced or depressed by $\boldsymbol{F}$, depending on the direction of $\boldsymbol{F}$ relative to the field direction. The D–A distance dependence, both of the electron transfer and of its field-induced change, is interpreted in terms of the electron tunneling through a potential barrier of a fatty acid monolayer.

Excimer formation process is shown to be influenced by $\boldsymbol{F}$ for pyrene doped in a PMMA film. The results show that electric fields induce a change in photochemical processes even when photoexcitation is not followed by a charge transfer. It is suggested that the electronic coupling is influenced by $\boldsymbol{F}$ with a field strength in the order of MV cm^{-1}, as a result of the orbital polarization.

As demonstrated in the methylene-linked compound where two pyrene chromophores are attached to the chain ends, i.e., 1,3-bis-(1-pyrenyl)propane, the measurements of the field effects on emission following photoirradiation are very useful to elucidate the mechanism of the efficient generation of electroluminescence. A radiative recombination of the hole-electron pair through a molecular chain may play a significant role in efficient generation of electroluminescence.

The present results imply that many photochemical processes can be controlled by $\boldsymbol{F}$. As the reaction mechanism of photosensitized enantiodifferentiating processes, a formation of a two diastereomeric exciplex pair between the excited sensitizer and substrate has been proposed,[91] and the exciplex formation between the substrate and chiral sensitizer is enhanced by $\boldsymbol{F}$.[92] Since the relative stability between the diastereomeric exciplexes is considered to be the major source of the enantioselectivity in the asymmetric photoreaction, it is anticipated in principle that not only the chemical yields but also the optical yields can be manipulated by $\boldsymbol{F}$. It should be also pointed out that other photoinduced dynamics such as proton transfer or excitation energy transfer (especially Dexter-type) may be also influenced significantly by an external electric field.

The author is grateful to all of the co-workers who contributed in this study. A part of this work was supported by Grants-in-Aid for Scientific Research from the Ministry of Education, Science, Sports and Culture.

References

1 C. H. Townes and A. L. Schawlow, “Microwave Spectroscopy,” McGraw-Hill, New York (1955), pp. 248–283.

2 A. D. Buckingham, in “Medical Technical Publishing Company International Review of Science: Physical Chemistry, Series 1,” ed by D. A. Ramsay, Butterworth, London (1972), Vol. 3, p. 73.

3 R. Hochstrasser, *Acc. Chem. Res.*, **6**, 263 (1973).

4 W. Liptay, in “Excited States,” ed by E. C. Lim, Academic Press, New York (1974), p. 129.

5 W. F. Polik, D. R. Guyer, and C. B. Moore, *J. Chem. Phys.*, **92**, 3453 (1990).

6 E. W. Schlag, W. E. Henke, and S. H. Lin, *Int. Rev. Phys. Chem.*, **2**, 43 (1982).

7 N. Ohta and T. Takemura, *Chem. Phys. Lett.*, **169**, 611 (1990).

8 D. E. Steiner and T. Ulrich, *Chem. Rev.*, **89**, 51 (1989).

9 “Dynamic Spin Chemistry,” ed by S. Nagakura, H. Hayashi, and T. Azumi, Kodansha/Wiley, Tokyo/New York (1998).

10 H. Hayashi, Y. Sakaguchi, and M. Wakasa, *Bull. Chem. Soc. Jpn.*, **74**, 773 (2001).

11 N. Ohta, *J. Phys. Chem.*, **100**, 7298 (1996).

12 R. B. Comizzori, *Photochem. Photobiol.*, **15**, 399 (1972).

13 M. Yokoyama, Y. Endo, and H. Mikawa, *Chem. Phys. Lett.*, **34**, 597 (1975); *Bull. Chem. Soc. Jpn.*, **49**, 1538 (1976).

14 M. Yokoyama, Y. Endo, A. Matsubara, and H. Mikawa, *J. Chem. Phys.*, **75**, 3006 (1981).

15 Z. D. Popovic, *Chem. Phys.*, **86**, 311 (1984).

16 P. D. Weisssand and M. Burberry, *Thin Solid Films*, **158**, 175 (1988).

17 H. Sakai, A. Itaya, and H. Masuhara, *J. Phys. Chem.*, **93**, 5351 (1989).

18 J. Kalinowski, W. Stampor, and P. G. Di Marco, *J. Chem. Phys.*, **96**, 4136 (1992).

19 N. Ohta, S. Umeuchi, Y. Nishimura, and I. Yamazaki, *J. Phys. Chem.*, **102**, 3784 (1998).

20 N. Pfeffer, D. Neher, M. Remmers, C. Poga, M. Hopmeier, and R. Mahrt, *Chem. Phys.*, **227**, 167 (1998).

21 Z. D. Popovic, M. I. Khan, S. J. Atherton, A.-M. Hor, and J. L. Goodman, *J. Phys. Chem. B*, **102**, 657 (1998).

22 D. Hertel, U. Scherf and H. Bössler, *Adv. Mater.*, **10**, 1119 (1998).

23 S. Yamaguchi and Y. Sasaki, *J. Phys. Chem. B*, **103**, 6835 (1999).

24 J. Jung, I. Glowacki, and J. Ulanski, *J. Chem. Phys.*, **110**, 7000 (1999).

25 J. Pan, U. Scherf, A. Schreiber, and D. Haarer, *J. Chem. Phys.*, **112**, 4305 (2000).

26 D. J. Lockhart and S. G. Boxer, *Chem. Phys. Lett.*, **144**, 243 (1988).

27 H. Kuhn, D. Möbius, and H. Bucher, in “Physical Methods

of Chemistry," ed by A. Weissberger and B. W. Rossiter, Wiley, New York (1972), Vol. 1, p. 577.

28 A. Ulman, "An Introduction to Ultrathin Organic Films from Langmuir–Blodgett to Self-Assembly," Academic Press, San Diego (1991).

29 H. Bücher, J. Wiegand, B. B. Snavely, K. H. Beck, and H. Kuhn, *Chem. Phys. Lett.*, **3**, 508 (1969).

30 H. Bücher and H. Kuhn, *Z. Naturforsch., B: Chem. Sci.*, **25**, 1312 (1970).

31 S. Nishikawa, Y. Tokura, T. Koda, and K. Iriyama, *Jpn. J. Appl. Phys.*, **25**, L701 (1986).

32 N. Ohta, S. Okazaki, and I. Yamazaki, *Chem. Phys. Lett.*, **229**, 394 (1994).

33 N. Ohta, T. Nomura, S. Okazaki, and I. Yamazaki, *Chem. Phys. Lett.*, **241**, 195 (1995).

34 N. Ohta, T. Ogata, S. Okazaki, and I. Yamazaki, *Chem. Phys. Lett.*, **244**, 355 (1995).

35 N. Ohta, M. Nakamura, I. Yamazaki, M. Shimomura, and K. Ijiro, *Langmuir*, **14**, 6226 (1998).

36 F. C. De Schryver, N. Boens, and J. Put, in "Adv. Photochem.," ed by J. N. Pitts, Jr., G. S. Hammond, and K. Gollnick, John Wiley & Sons, New York (1977), Vol. 10, p. 359.

37 a) P. Pasman, F. Rob, and J. W. Verhoeven, *J. Am. Chem. Soc.*, **104**, 5127 (1982). b) M. N. Paddon-Row, A. M. Oliver, J. M. Warman, K. J. Smit, M. P. de Haas, H. Oevering, and J. W. Verhoeven, *J. Phys. Chem.*, **92**, 6958 (1988).

38 N. Mataga, *Pure Appl. Chem.*, **56**, 1255 (1984).

39 M. R. Wasielewski, *Chem. Rev.*, **92**, 435 (1992).

40 S. G. Boxer, in "The Photosynthetic Reaction Center," ed by J. Deisenhofer and J. R. Norris, Academic Press, Sandiego (1993), Vol. II, p. 179.

41 M. Ponder and R. Mathies, *J. Phys. Chem.*, **87**, 5090 (1983).

42 S. Abe, Y. Nishimura, I. Yamazaki, and N. Ohta, *Asian J. Spectrosc.*, **4**, 105 (1999).

43 N. Ohta, Y. Iwaki, T. Ito, I. Yamazaki, and A. Osuka, *J. Phys. Chem. B*, **103**, 11242 (1999).

44 Y. Iwaki and N. Ohta, *Chem. Lett.*, **2000**, 894.

45 N. Ohta, T. Tanaka, and I. Yamazaki, *Res. Chem. Intermed.*, **27**, 61 (2001).

46 G. U. Bublitz and S. G. Boxer, *Ann. Rev. Phys. Chem.*, **48**, 213 (1997)

47 W. Baumann and H. Bischof, *J. Mol. Struct.*, **129**, 125 (1985).

48 N. Ohta, T. Kanada, I. Yamazaki, S. Ito, and I. Suzuka, *J. Lumin.*, **79**, 177 (1998).

49 D. J. Lockhart, S. L. Hammes, S. Franzen, and S. G. Boxer, *J. Phys. Chem.*, **95**, 2217 (1991).

50 S. Umeuchi, Y. Nishimura, I. Yamazaki, H. Murakami, M. Yamashita, and N. Ohta, *Thin Solid Films*, **311**, 239 (1997).

51 N. Ohta, T. Ito, S. Okazaki, and I. Yamazaki, *J. Phys. Chem. B*, **101**, 10213 (1997).

52 P. Fromherz, U. Oelschlägel, and W. Wilke, *Thin Solid Films*, **159**, 421 (1988).

53 N. Ohta, N. Tamai, T. Kuroda, T. Yamazaki, Y. Nishimura, and I. Yamazaki, *Chem. Phys.*, **177**, 591 (1993).

54 R. A. Marcus, *J. Chem. Phys.*, **24**, 966 (1956); *Ann. Rev. Phys. Chem.*, **15**, 155 (1964).

55 R. A. Marcus and N. Sutin, *Biochim. Biophys. Acta*, **811**, 265 (1985).

56 C. C. Moser, J. M. Keske, K. Warncke, R. S. Farid, and P. L. Dutton, *Nature*, **355**, 796 (1992).

57 N. Ohta, M. Koizumi, S. Umeuchi, Y. Nishimura, and I. Yamazaki, *J. Phys. Chem.*, **100**, 16466 (1996).

58 A. Sillen and Y. Engelborghs, *Photochem. Photobiol.*, **67**, 475 (1998)

59 G. L. Closs, L. T. Calcaterra, N. J. Green, K. W. Penfield, and J. R. Miller, *J. Phys. Chem.*, **90**, 3673 (1986).

60 Y. Nishimura, I. Yamazaki, and N. Ohta, *J. Lumin.*, **87-89**, 791 (2000).

61 M. Hilczer, S. Traytak, and M. Tachiya, *J. Chem. Phys.*, **115**, 11249 (2001).

62 "Polymer Handbook," ed by J. Brandrup and E. H. Immergut; John Willey & Sons, New York (1975).

63 M. Tachiya and S. Murata, *J. Phys. Chem.*, **96**, 8441 (1992).

64 H. Kawabata, N. Ohta, H. Arakawa, M. Ashida, S. Kohtani, and R. Nakagaki, *J. Chem. Phys.*, **114**, 7723 (2001).

65 N. Ohta, M. Koizumi, Y. Nishimura, I. Yamazaki, Y. Tanimoto, Y. Hatano, M. Yamamoto, and H. Kono, *J. Phys. Chem.*, **100**, 19295 (1996).

66 Y. Nishimura, N. Ohta, M. Yamamoto, and I. Yamazaki, *Mol. Crys. Liq. Crys.*, **315**, 181 (1998).

67 N. Ohta, T. Kanada, I. Yamazaki, and M. Itoh, *Chem. Phys. Lett.*, **292**, 535 (1998).

68 Y. Nishimura, I. Yamazaki, M. Yamamoto, and N. Ohta, *Chem. Phys. Lett.*, **307**, 8 (1999).

69 T. Kanada, Y. Nishimura, I. Yamazaki, M. Yamamoto, and N. Ohta, *Chem. Phys. Lett.*, **332**, 442 (2000).

70 H. Kawabata, Y. Nishimura, I. Yamazaki, K. Iwai, and N. Ohta, *J. Phys. Chem.*, **105**, 10261 (2001).

71 M. Tachiya (private communication). According to a theoretical work, electron transfer rate can be enhanced or deenhanced by an electric field, depending both on the donor-acceptor distance and on the free energy gap for reaction. See also reference 61.

72 T. Ito, I. Yamazaki, and N. Ohta, *Chem. Phys. Lett.*, **277**, 125 (1997).

73 H. Kuhn, *J. Photochem.*, **10**, 111 (1979).

74 D. Möbius, Ber. Bunsenges. *Phys. Chem.*, **82**, 848 (1978); *Acc. Chem. Res.*, **14**, 63 (1981).

75 H. Kuhn, in "Proc. Robert A. Welch Found. Conf. Chem. Res. XXX, Advances in Electrochemistry, Houston, TX," (1986) p. 338.

76 N. Ohta, T. Ito, and I. Yamazaki, *Z. Phys. Chem.*, **213**, Part II, 191 (1999).

77 B. Mann and H. Kuhn, *J. Appl. Phys.*, **42**, 4398 (1971).

78 H. Kuhn and D. Möbius, in "Investigations of Surfaces and Interfaces, Part B," ed by B. W. Rossiter and R. C. Baetzold, Physical Methods of Chemistry Series, John Willey & Sons (1993), Vol. IXB, Chap. 6, p. 375.

79 T. Miyashita, Y. Hasegawa, and M. Matsuda, *J. Phys. Chem.*, **96**, 2790 (1992).

80 T. Ito, I. Yamazaki, and N. Ohta, *J. Phys. Chem. B*, **106**, 895 (2002).

81 N. Ohta, T. Ito, and I. Yamazaki, *Mol. Crys. Liq. Crys.*, **314**, 119 (1998).

82 N. Ohta, T. Nomura, and I. Yamazaki, *J. Photochem. Photobiol.*, **106**, 37 (1997).

83 N. Ohta, S. Umeuchi, T. Kanada, Y. Nishimura, and I. Yamazaki, *Chem. Phys. Lett.*, **277**, 215 (1997).

84 H. Port, R. Seyfang, and H. C. Wolf, *J. Phys. C*, C7-391 (1985).

85 A. Matsui, K. Mizuno, N. Tamai, and I. Yamazaki, *Chem. Phys.*, **113**, 111 (1987).

86 I. Yamazaki, N. Tamai, and T. Yamazaki, *J. Phys. Chem.*, **91**, 3572 (1987).
87 M. Mitsuya, Y. Taniguchi, N. Tamai, I. Yamazaki, and H. Masuhara, *Thin Solid Films*, **129**, L45 (1985).
88 R. Horiguchi, N. Iwasaki, and Y. Maruyama, *J. Phys. Chem.*, **91**, 5135 (1987).
89 A. Matsui, T. Ohno, K. Mizuno, T. Yokoyama, and M. Kobayashi, *Chem. Phys.*, **111**, 121 (1987).
90 N. Ohta, H. Kawabata, S. Umeuchi, and I. Yamazaki, *Chem. Phys. Lett.*, **310**, 397 (1999); **315**, 151 (1999).
91 S. Asaoka, T. Kitazawa, T. Wada, and Y. Inoue, *J. Am. Chem. Soc.*, **121**, 8486 (1999).
92 Y. Takehara, N. Ohta, S. Shiraishi, S. Asaoka, T. Wada, and Y. Inoue, *J. Photochem. Photobiol. A: Chemistry*, **145**, 53 (2001).

Nobuhiro Ohta was born in Tendo, Yamagata Prefecture, Japan in 1950. He has received his Ph.D. degree from Tohoku University in 1977. He worked as a postdoctoral fellow at Marquette University in Milwaukee for one year. He was appointed research associate in the Research Institute of Applied Electricity at Hokkaido University in 1978. He was appointed associate professor in the Faculty of Engineering at the same university in 1992. Since 1998, he has been a professor in the Research Institute for Electronic Science (RIES) at Hokkaido University. He received the Japanese Photochemistry Award in 1998 and the Divisional Award of the Chemical Society of Japan in 2001. His research interests are in structure and dynamics of molecules and molecular systems following photoexcitation and in their relation with photoinduced function of materials. Electric field and magnetic field are particularly applied as an external perturbation in order to elucidate the relations among structure, dynamics and photoinduced function.